UNIVERSITY of VIRGINIA
ORTHOPAEDIC SURGERY

Challenges in Treating Large Bone Defect

Quanjun (Trey) Cui, MD
Professor and Vice Chair for Research

Department of Orthopaedic Surgery

Faculty Research Retreat

April 23, 2016

Statistics and cost of fracture

- **7.9 million fractures/year** in the United States, 5% to 20% result in delayed or impaired healing J Bone Miner Res. 2010. 25:404-414
- Mean total costs per patient per year for fractures of the hip ($26,856), femur ($14,805), tibia ($10,224), and pelvis ($10,198) Osteoporosis Int. 2006. 17:252-258
- The average annual total **direct costs** of care for musculoskeletal diseases (spinal conditions, osteoarthritis, fractures) were estimated at **$510 billion** JAMA. 2009. 302:1586-1587
- **Indirect annual costs** from lost wages among persons aged 18 to 64 years having musculoskeletal diseases (spinal conditions, osteoarthritis, fractures) were estimated **at $330 billion** JAMA. 2009. 302:1586-1587

Orthopaedic Surgeon on Call

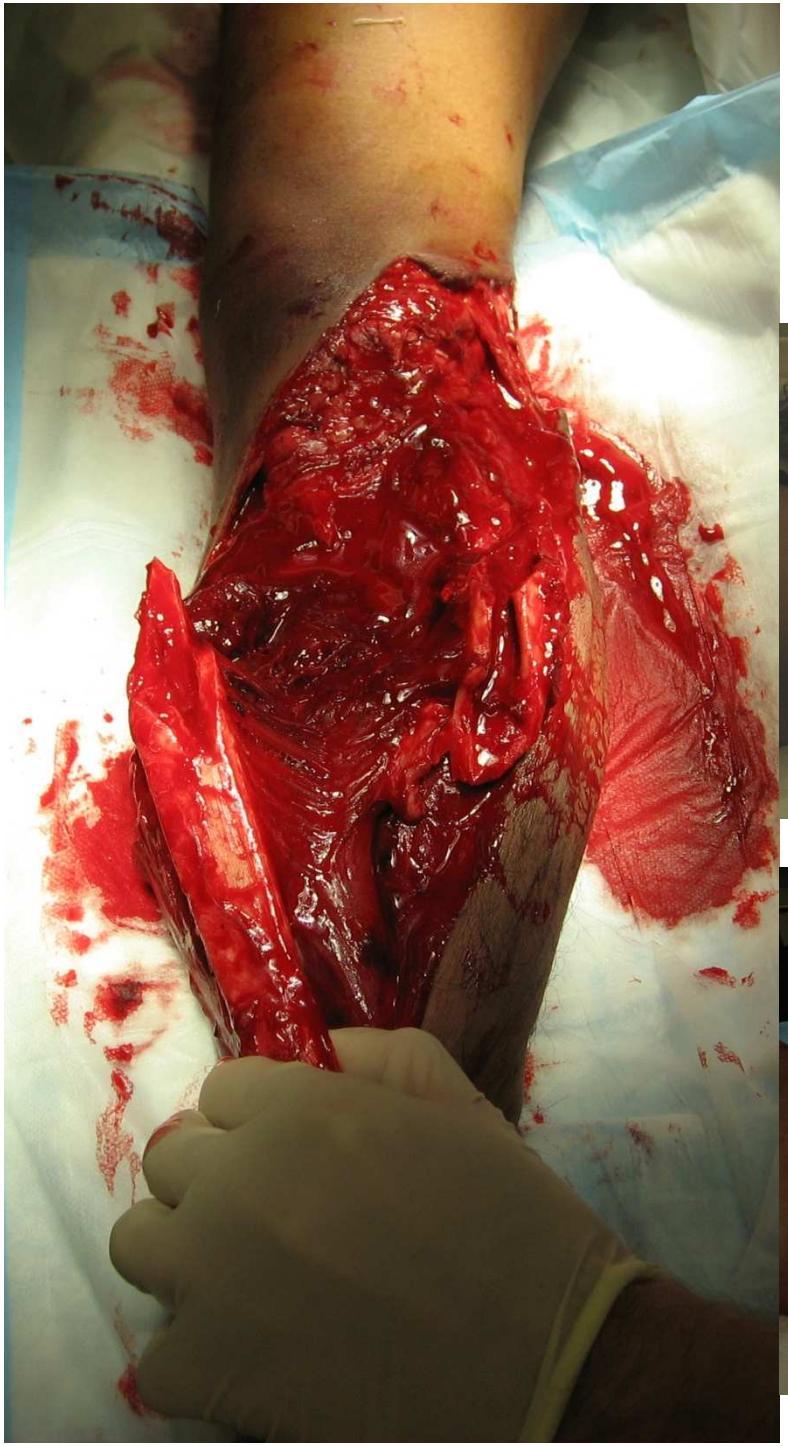

Case #1

28 yo M s/p peds vs car

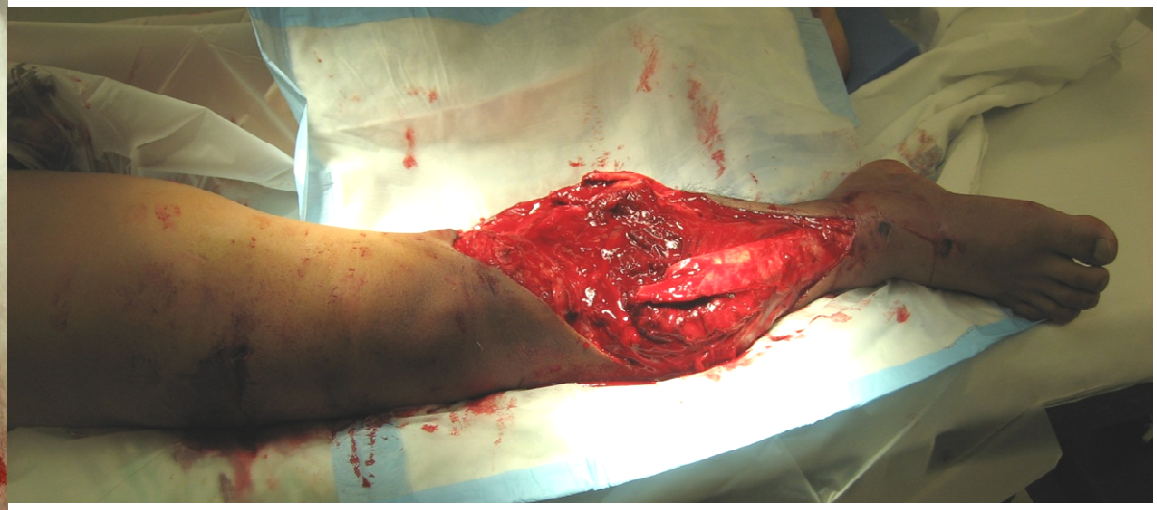

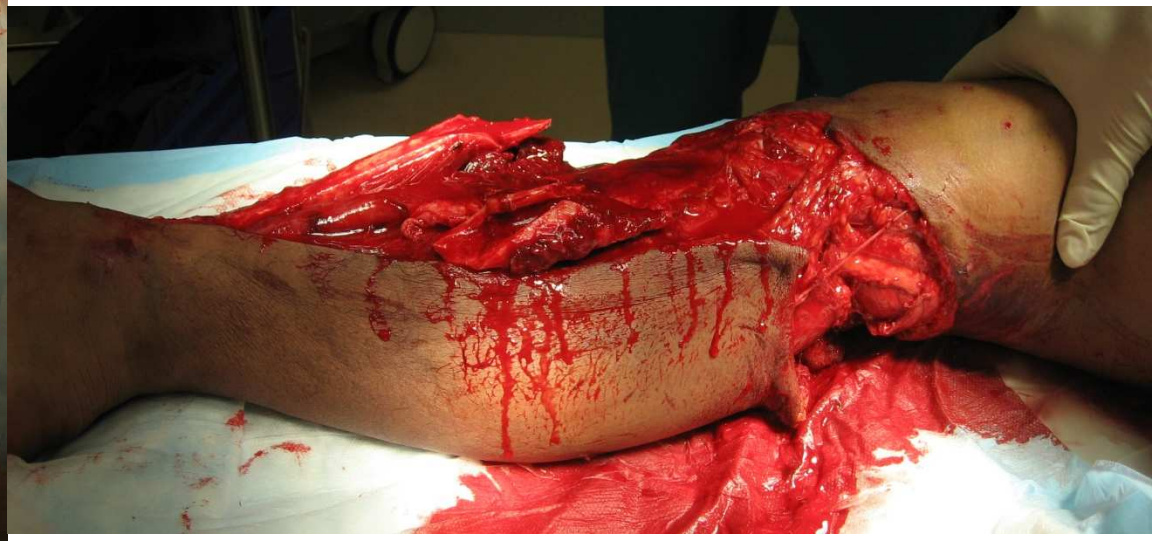

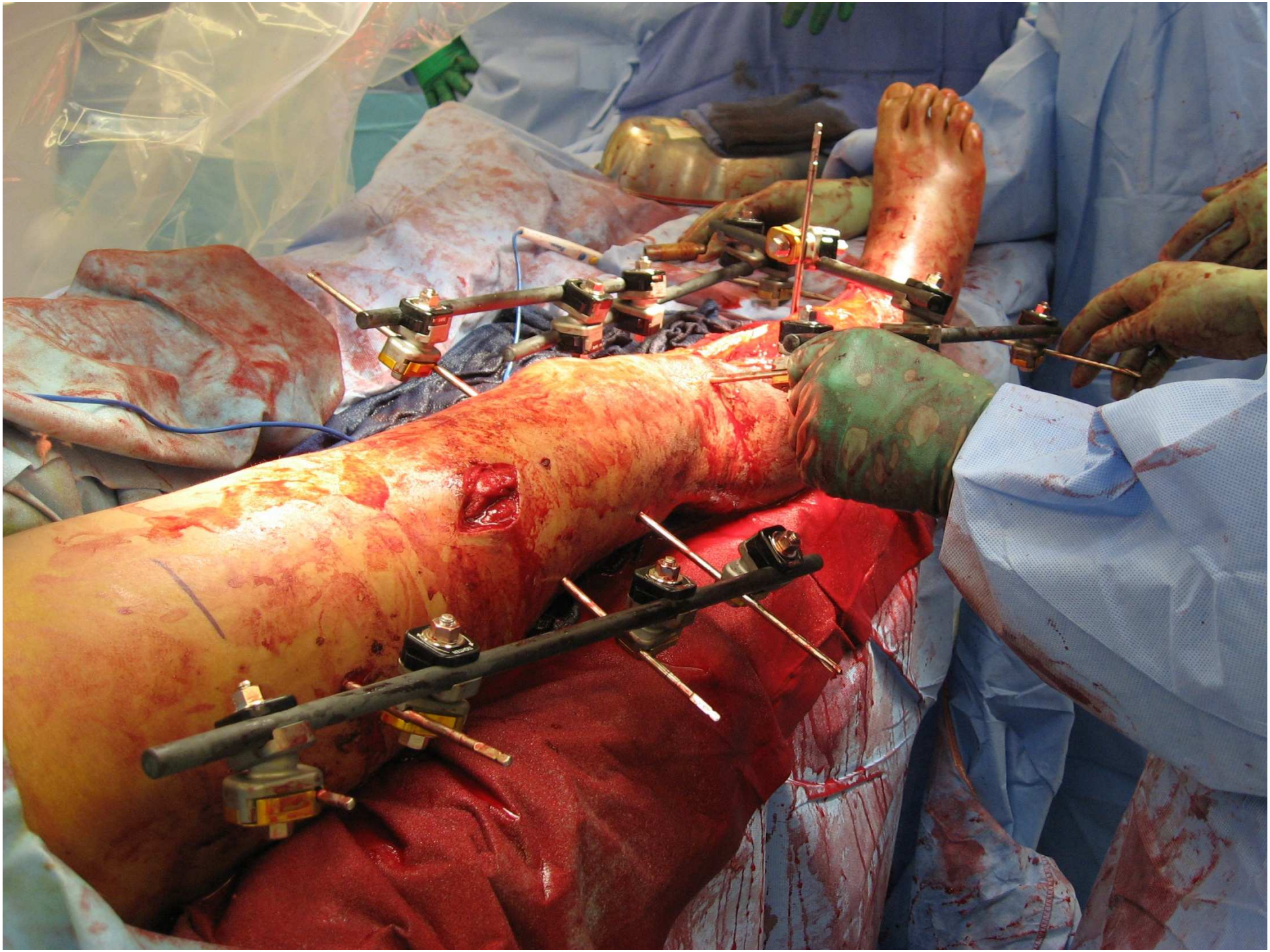

R
PORTAB
S/P EX

R
2\b EX-LIX

Case #2, failed ORIF of hip fracture

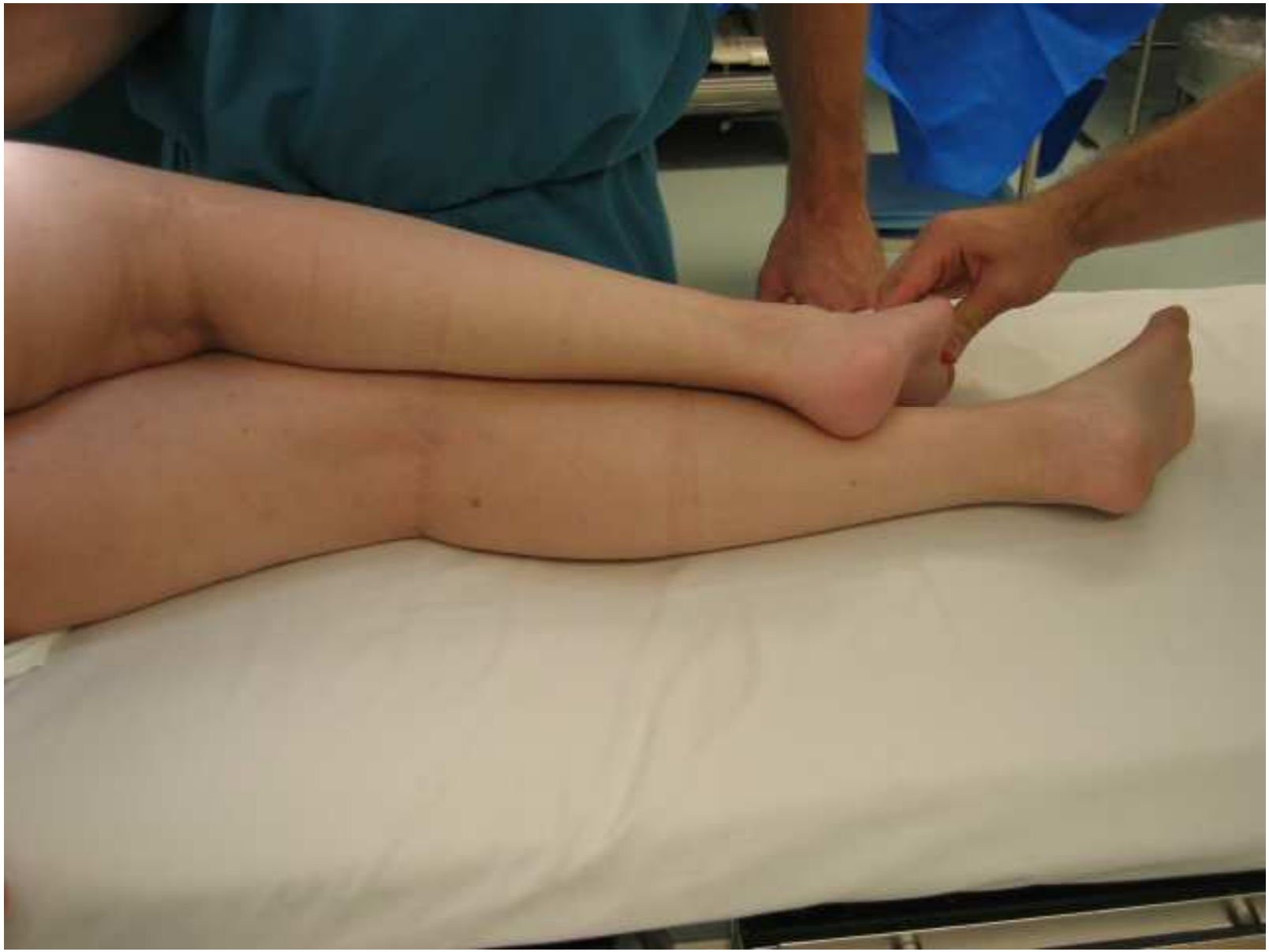

Case #2, failed ORIF of hip fracture

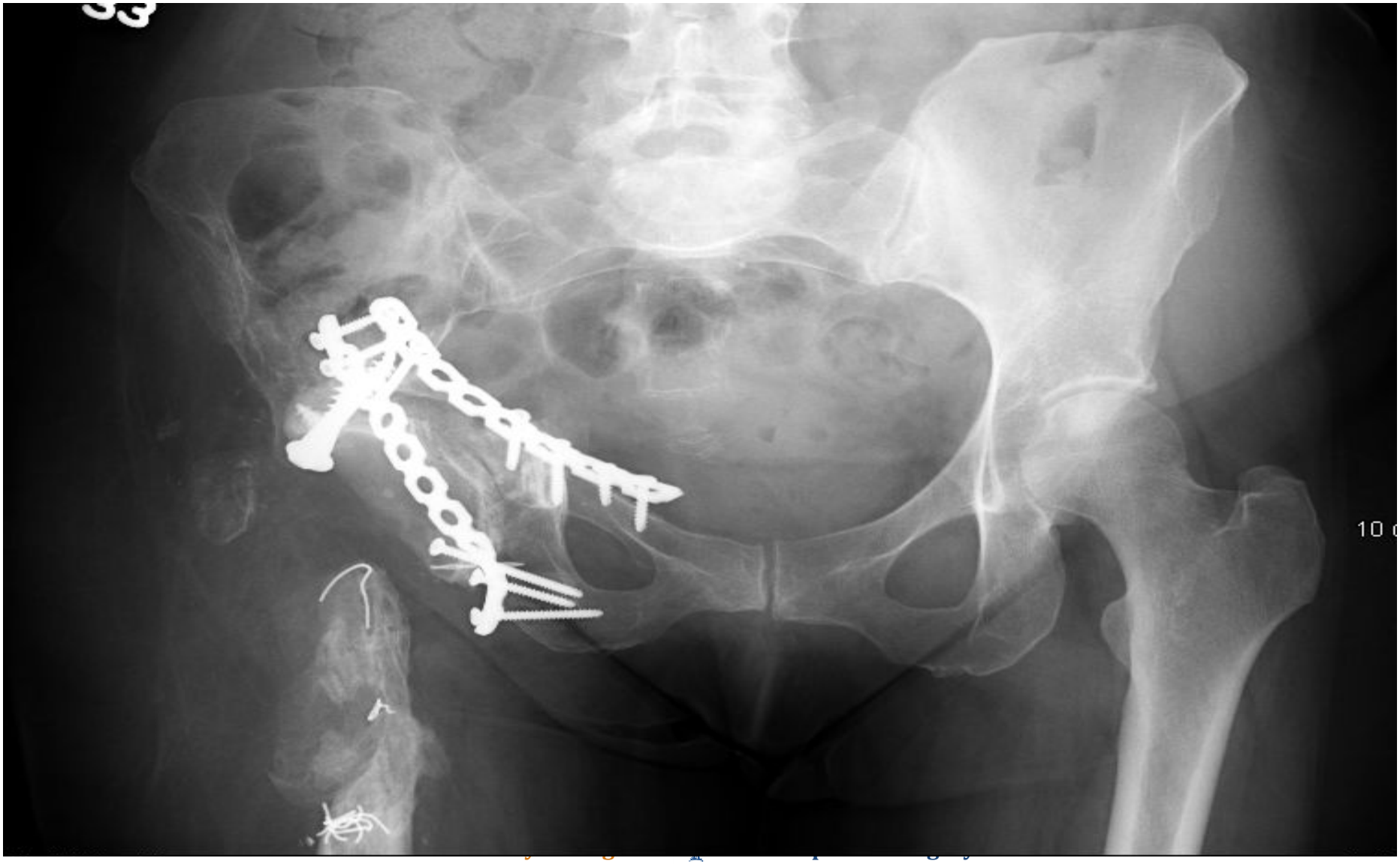

Case #2, failed ORIF of hip fracture

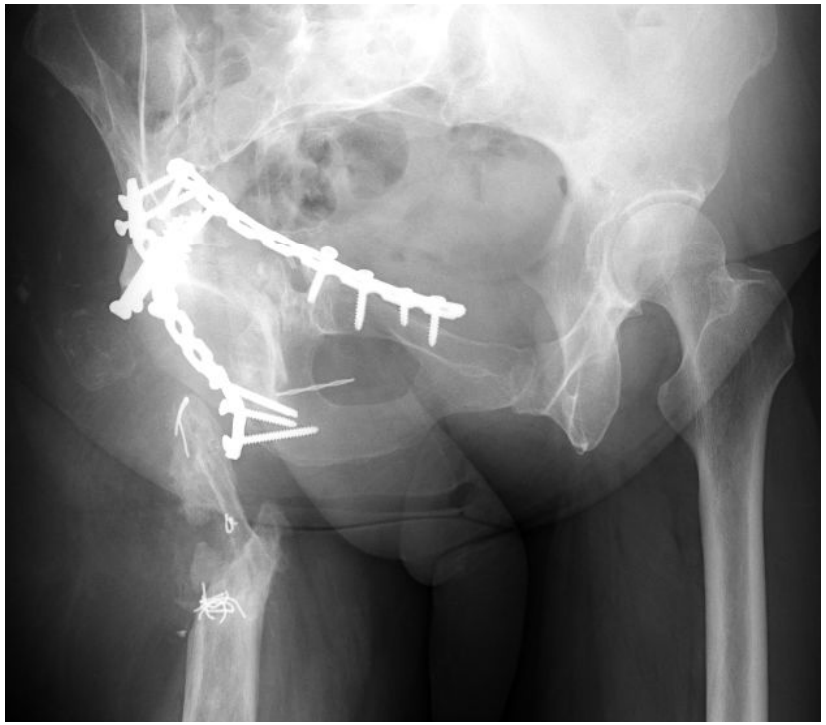

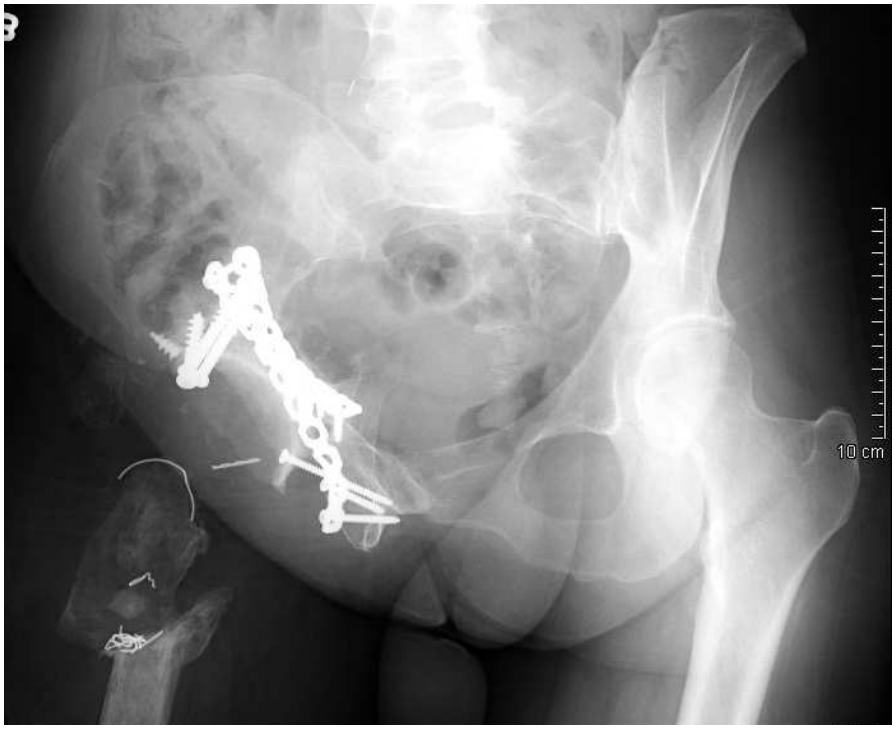

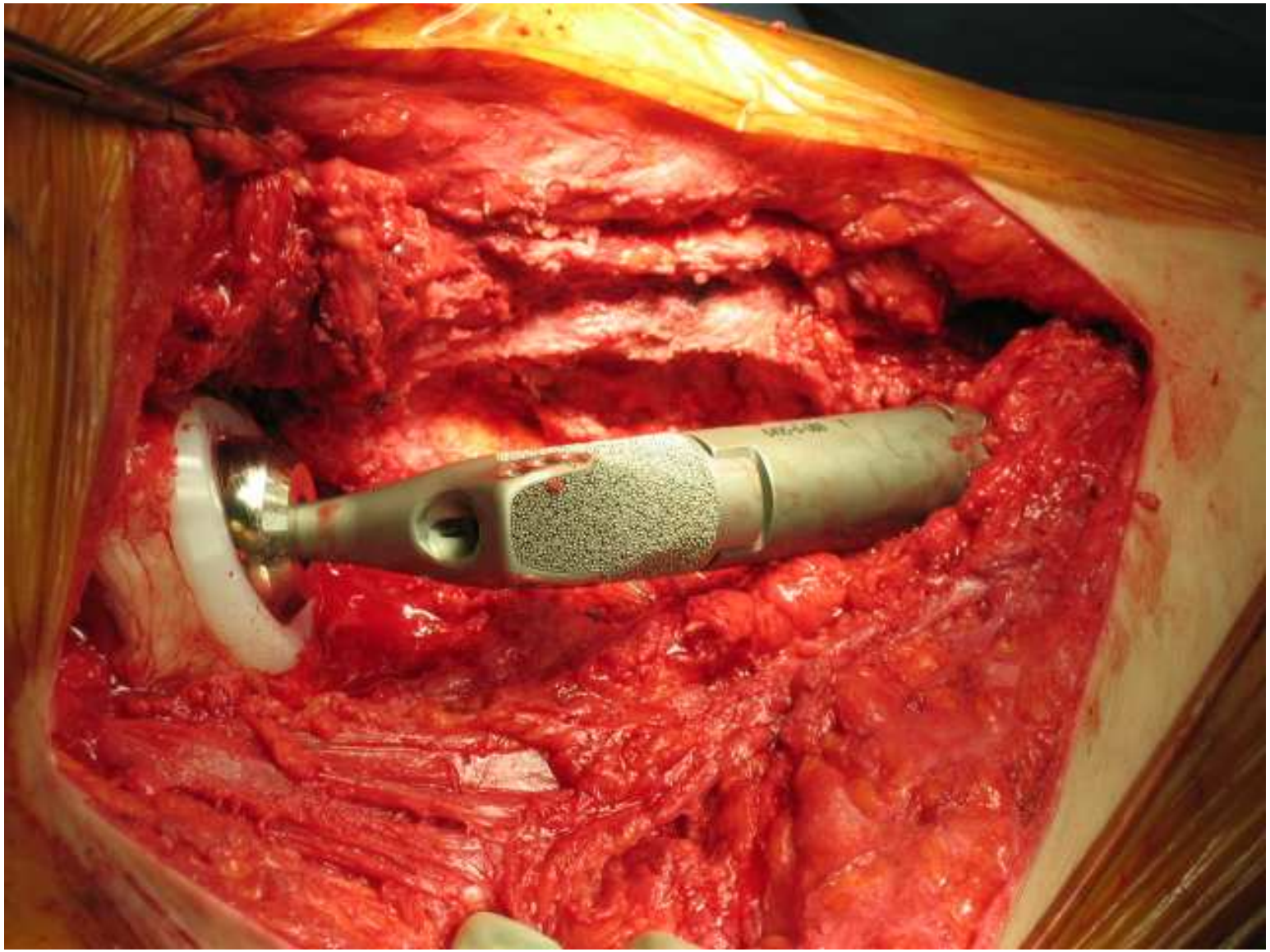

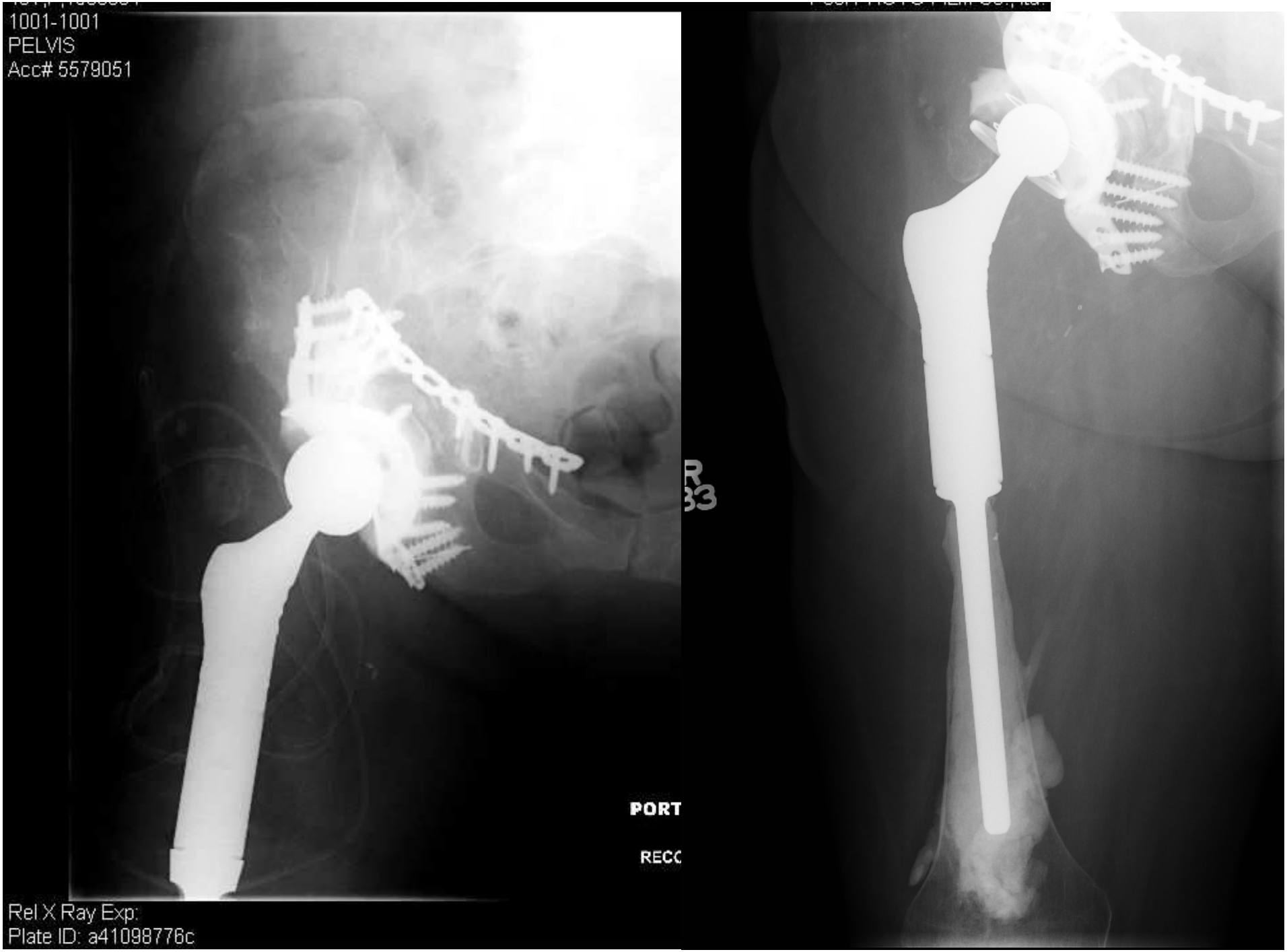
1001-1001
PELVIS
Acc# 5579051
PORT
RECC
Rel X Ray Exp:
Plate ID: a41098776c

So what's next?

Story is not over yet!!

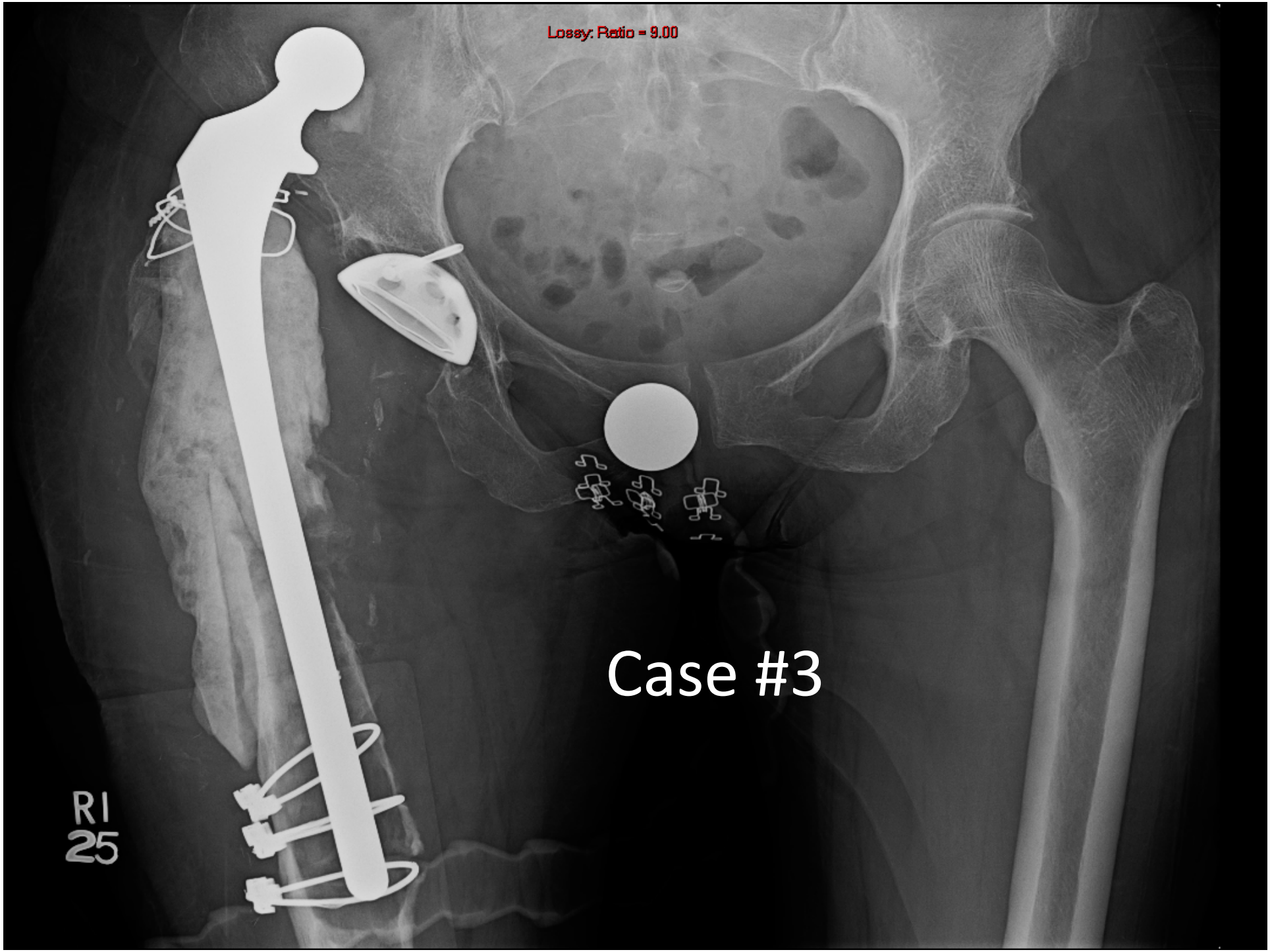
Lossy: Ratio = 9.00
Case #3
RI
25

Case #3

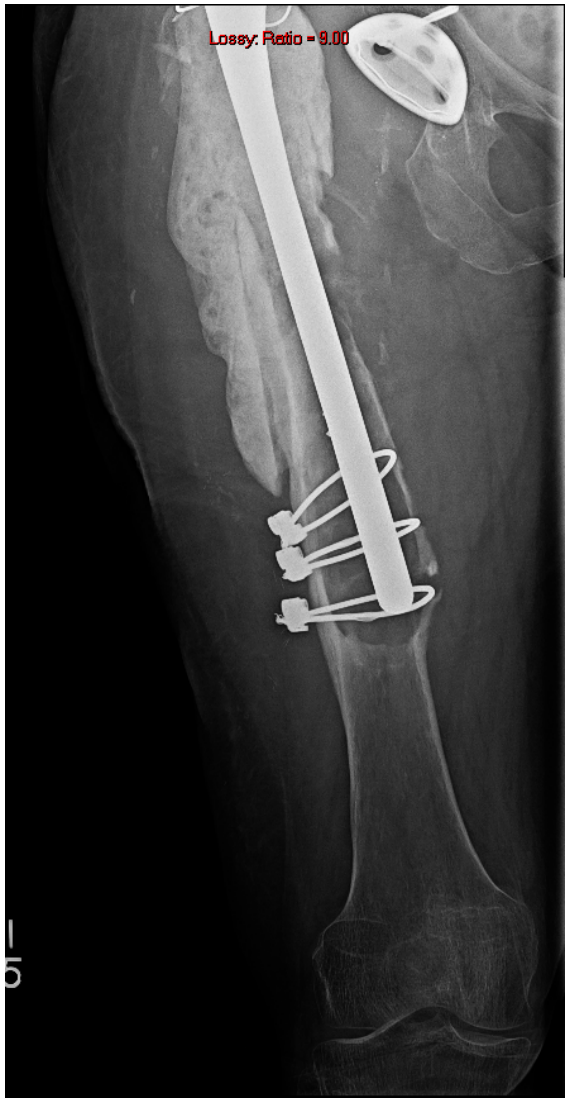

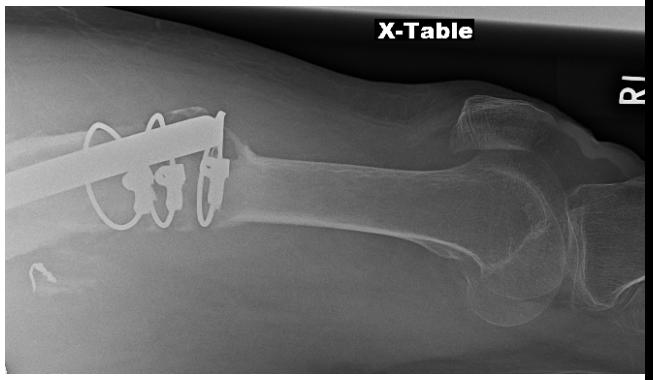

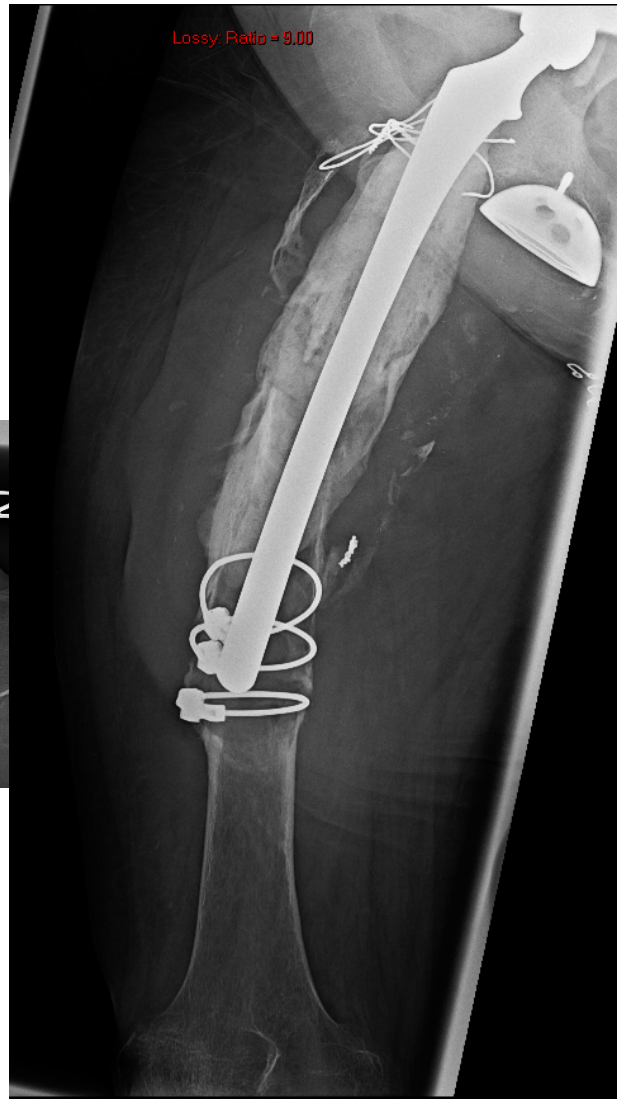

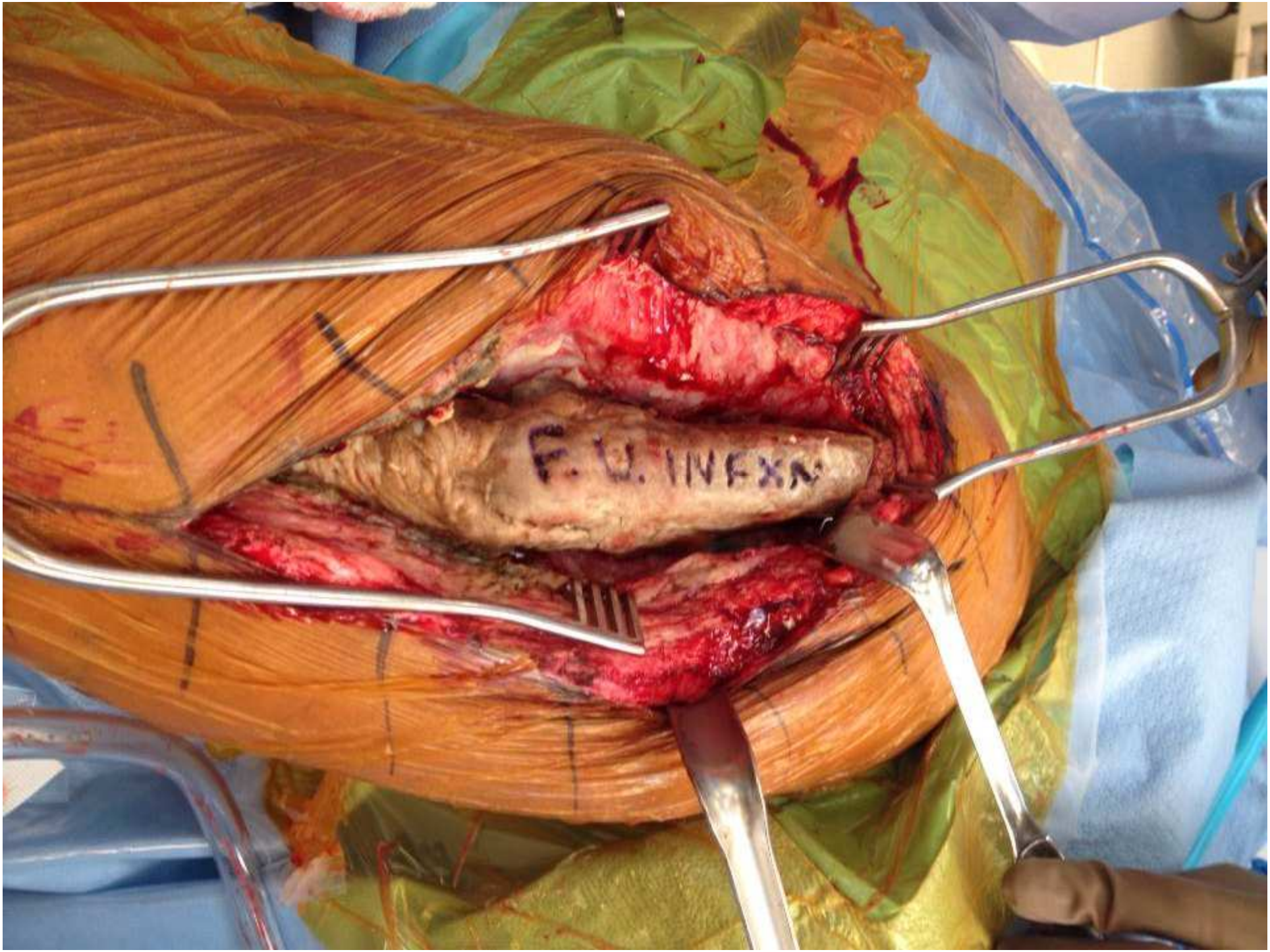
F. U. INFXN

Case #3

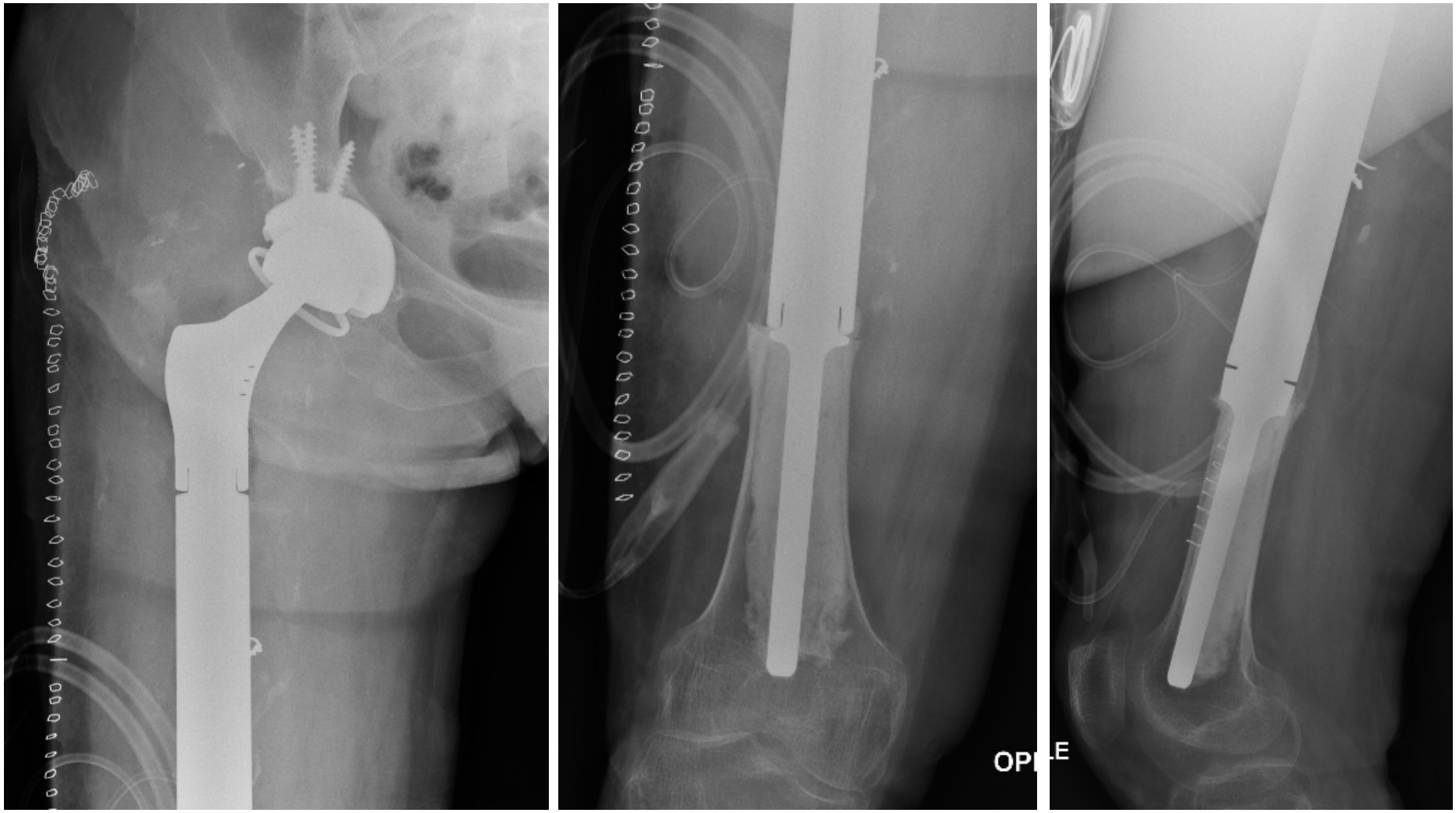

Case #4 Osteonecrosis

40 yo female presents with right hip pain ?

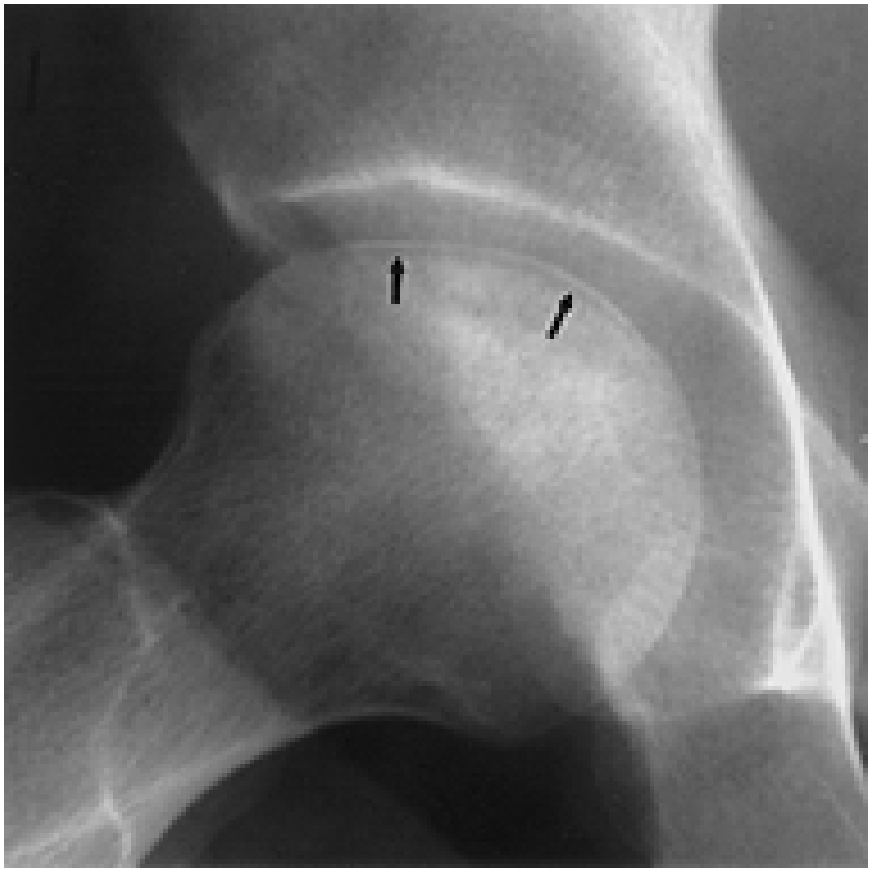

- Diagnosis ?
- Stage ?
- Pathology?

Case #4 Osteonecrosis

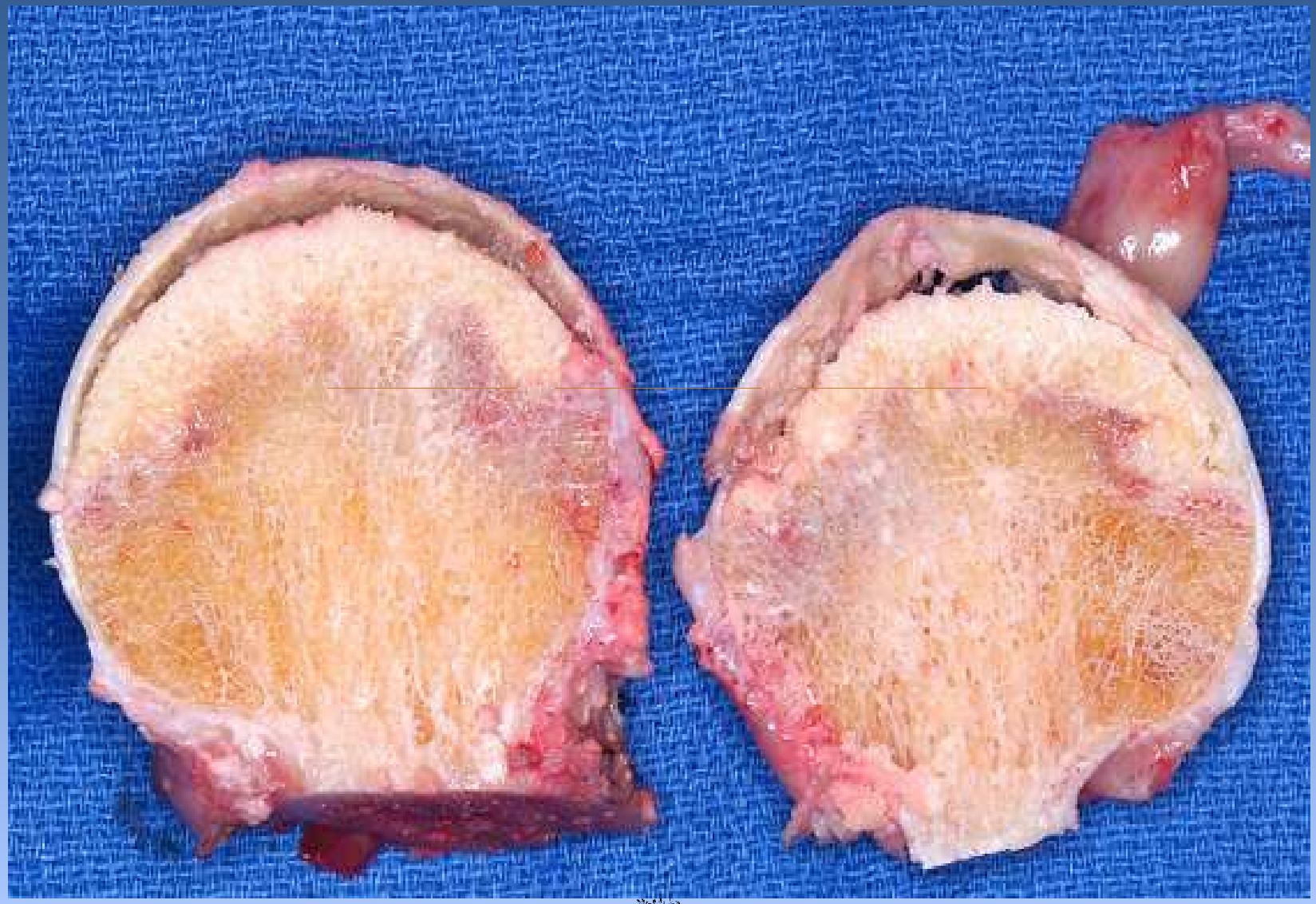

Case #5 Osteonecrosis

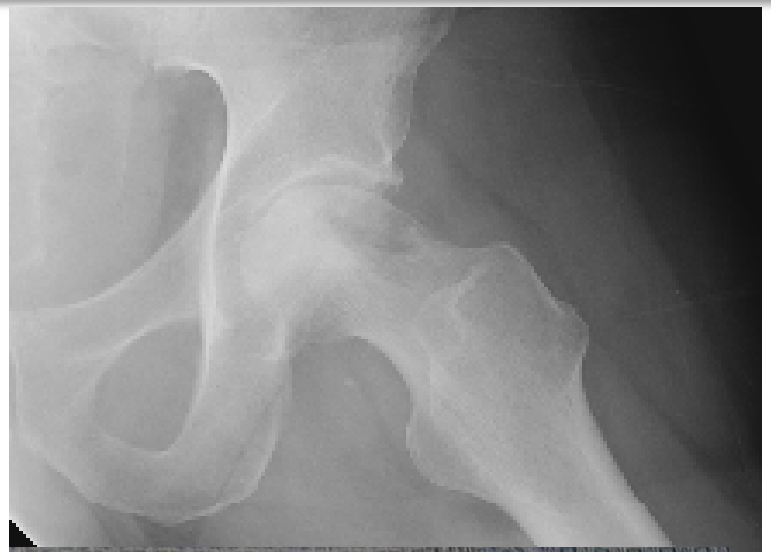

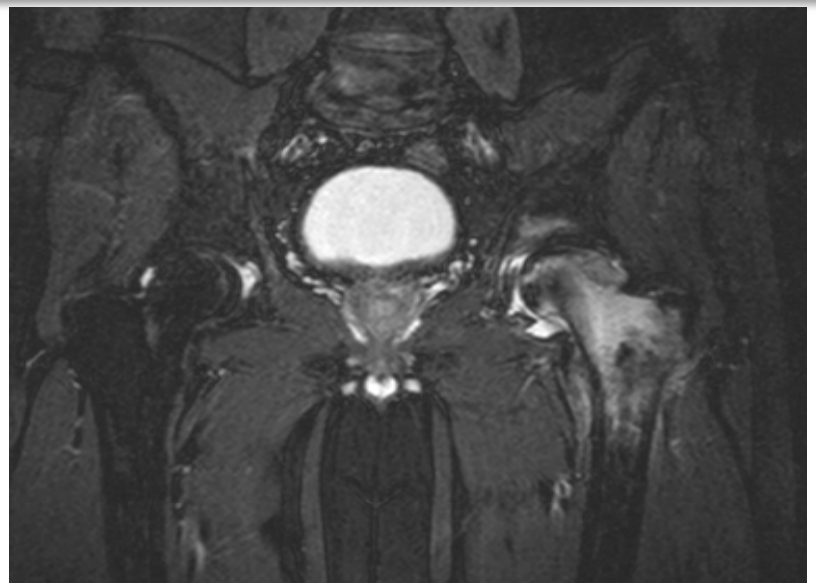

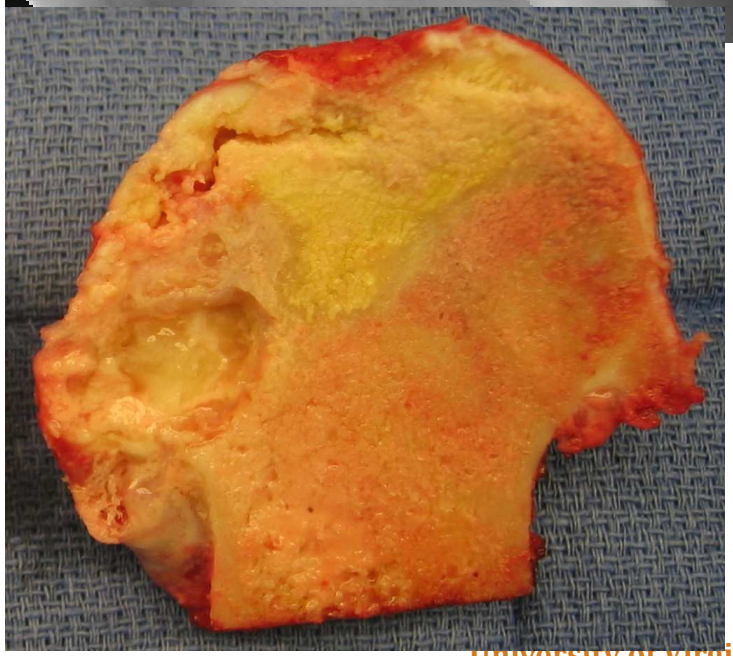

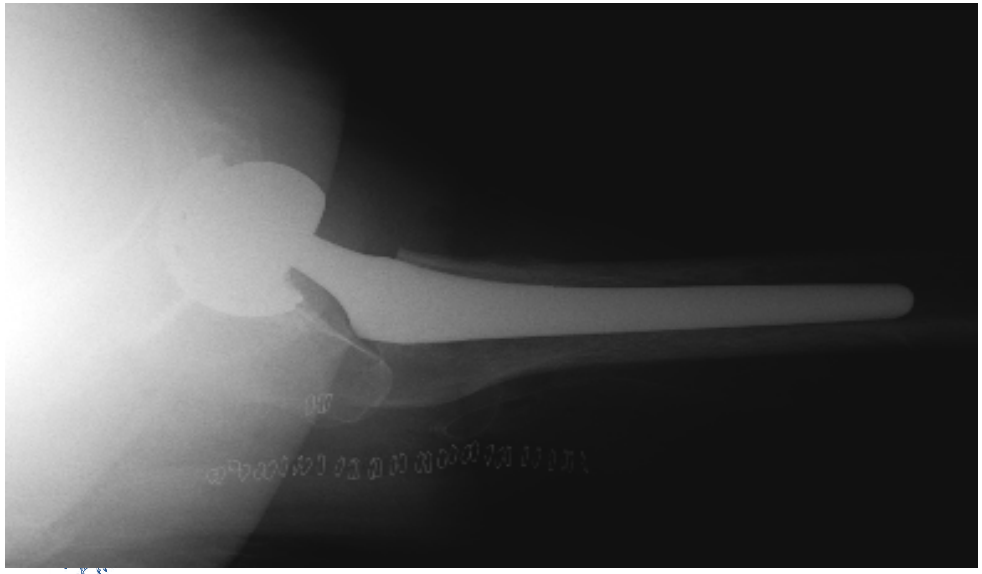

Core decompression + MSCs

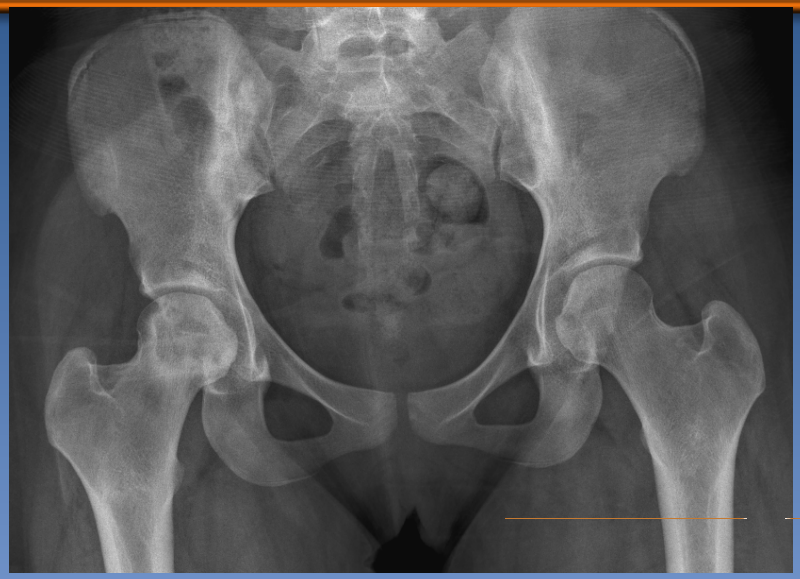

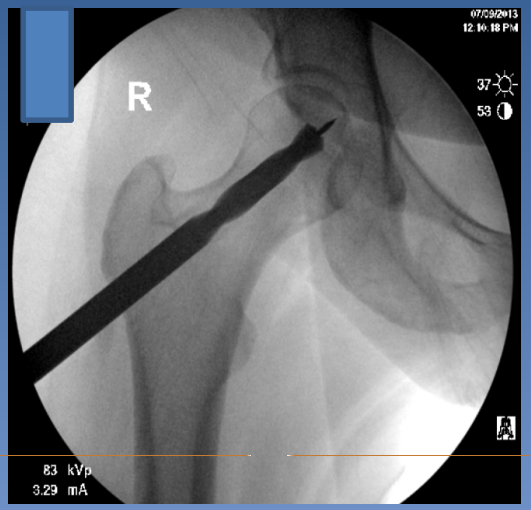

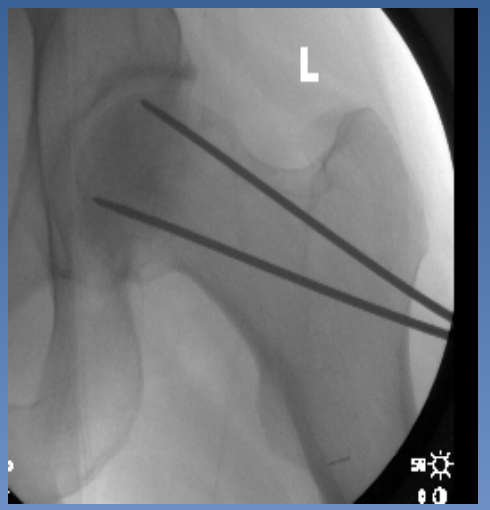

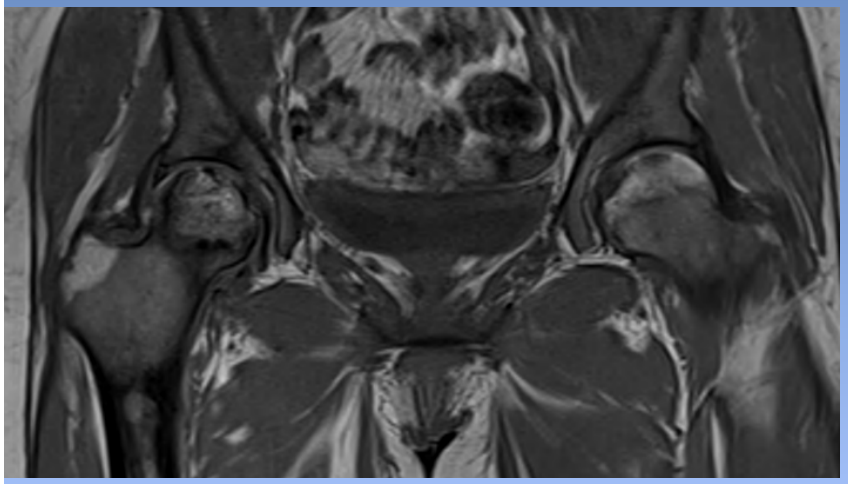

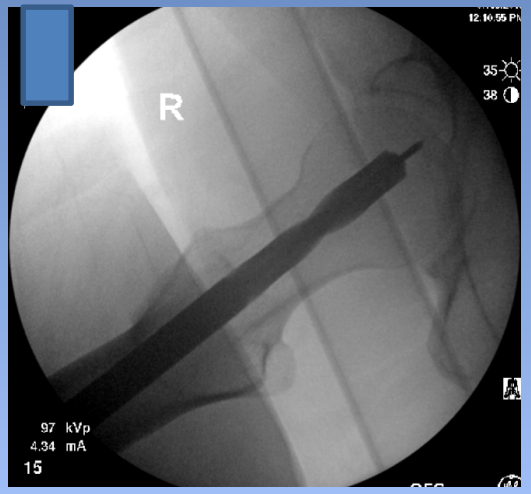

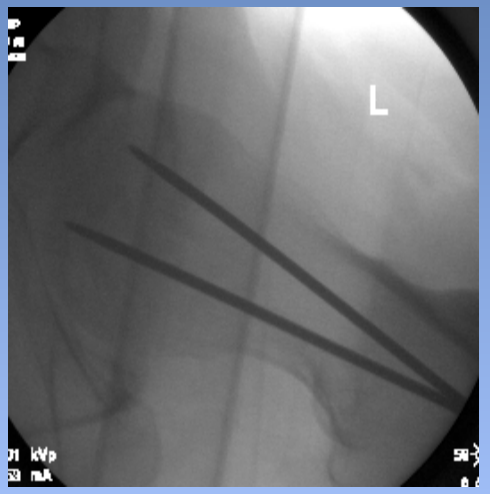

Bone marrow concentrates:

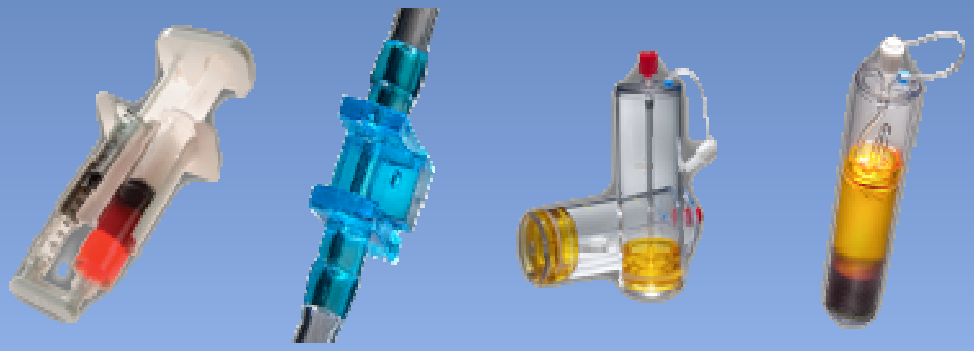

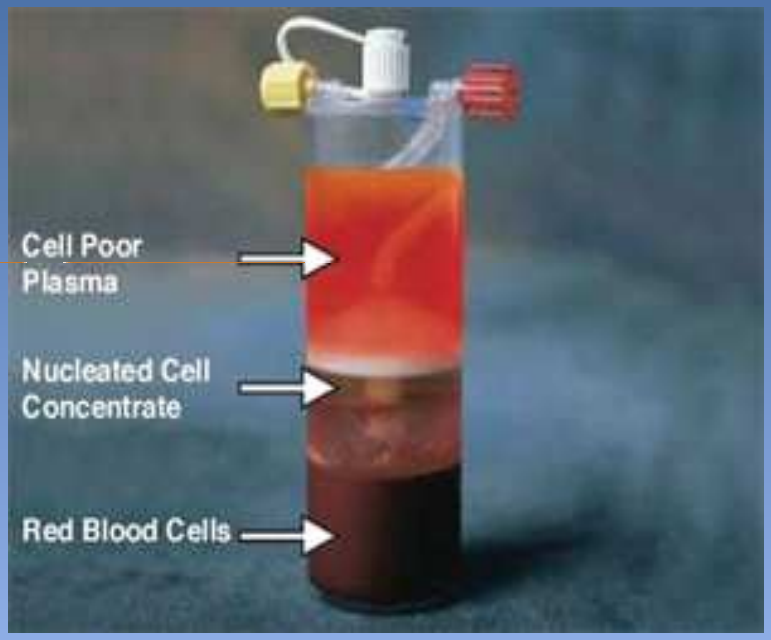

Hernigou, et al: CORR 2002; ARCO 2013
Gangji V, Toungouz M, Hauzeur JP. Expert Opin Biol Ther 2005;5(4):437-42
Gangji V, et al. J Bone Joint Surg Am 2004;86-A(6):1153-60


02/11/2014 08:44


02/11/2014 08:45


02/11/2014 09:00


Safe Surg Checklist
02/11/2014 09:02

Why study MSCs? Clinically speaking -

A REALITY CHECK

It is estimated that more than 500,000 bone-grafting procedures are performed annually in the United States, with approximately half of these procedures related to spine fusion. These numbers easily double on a global basis and indicate a shortage in the availability of musculoskeletal donor tissue traditionally used in these reconstructions. (Figure 1)

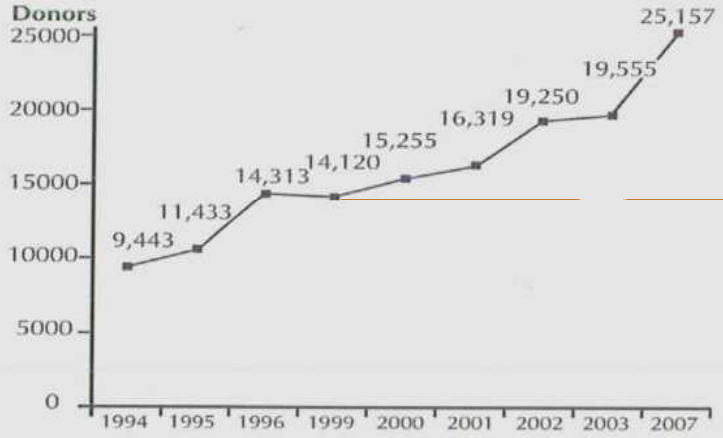

Figure 1: *U.S. trends in musculoskeletal tissue donors. Source: AATB Annual Survey*

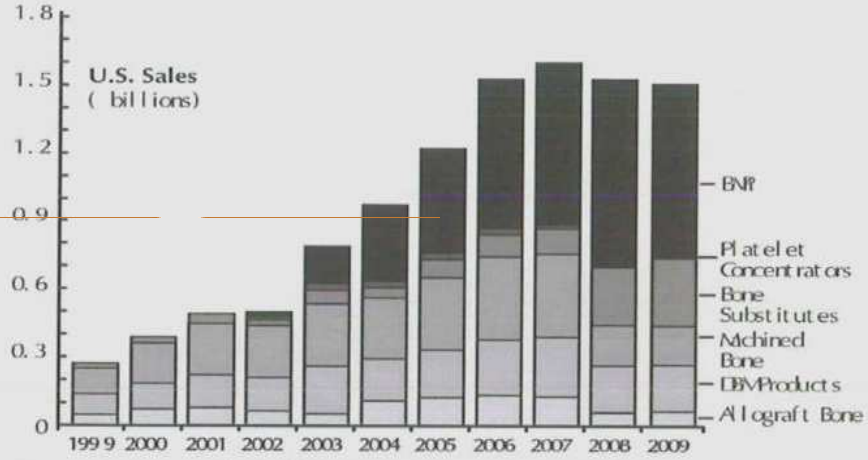

Figure 2: *U.S. sales of bone graft and bone-graft substitutes Source: Orthopedic Network News*

This reality has stimulated a proliferation of corporate interest in supplying what is seen as a growing market in bone replacement materials. (Figure 2) These graft alternatives are subjected to varying degrees of regulatory scrutiny, and thus their true effectiveness in patients may not be known prior to their use by orthopaedic surgeons. It is important to gain insight into this emerging class of bone-graft alternatives.

Evidence based medicine ?

Another Milestone in Medicine ?

What is the problem?

Autograft bone – supply limited

Allograft bone – immune/disease transmission

Bone graft substitutes – not ideal

Growth factors – Timing, doses, location?

Tissue-engineered large bone graft: Mechanical strength? Blood supply? Incorporation (rejection)?

Scaffold – cells – growth factors (soil-seeds-water): many studies focus on one factor

Hypothesis

VEGF may interact synergistically with **BMP** to enhance bone formation and angiogenesis mediated by bone marrow stem cells

BMP-6 used in our study

von-Kossa staining of stem cell

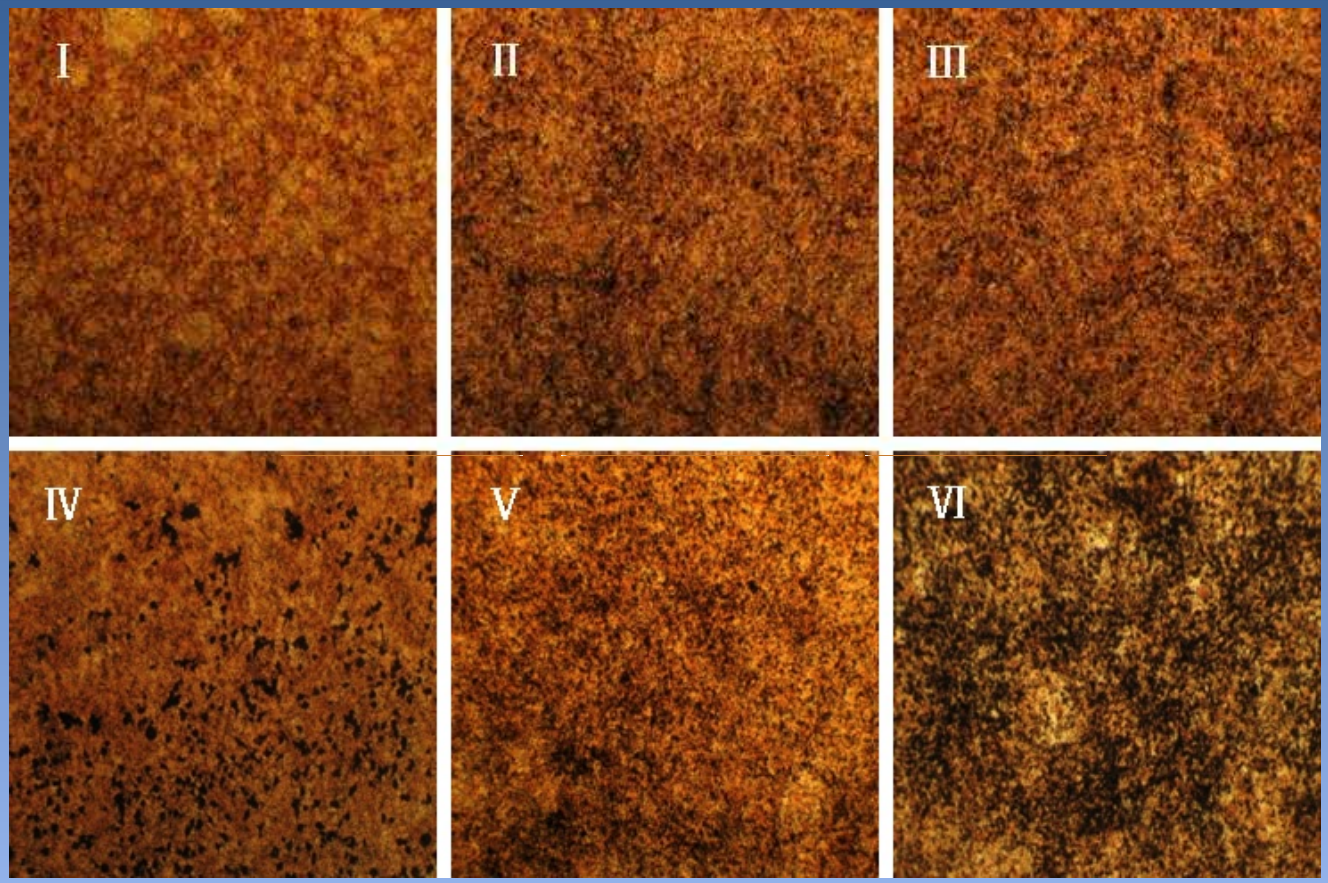

von-Kossa stain showing mineralization of non-transfected and transfected D1 cells after 14 days of growth in the culture medium. (Ⅰ) BM, (Ⅱ) OM, (Ⅲ) pN, (Ⅳ) pB6, (Ⅴ) pV, (Ⅵ) pVB6.

Quantification of mRNAs by

real-time quantitative PCR

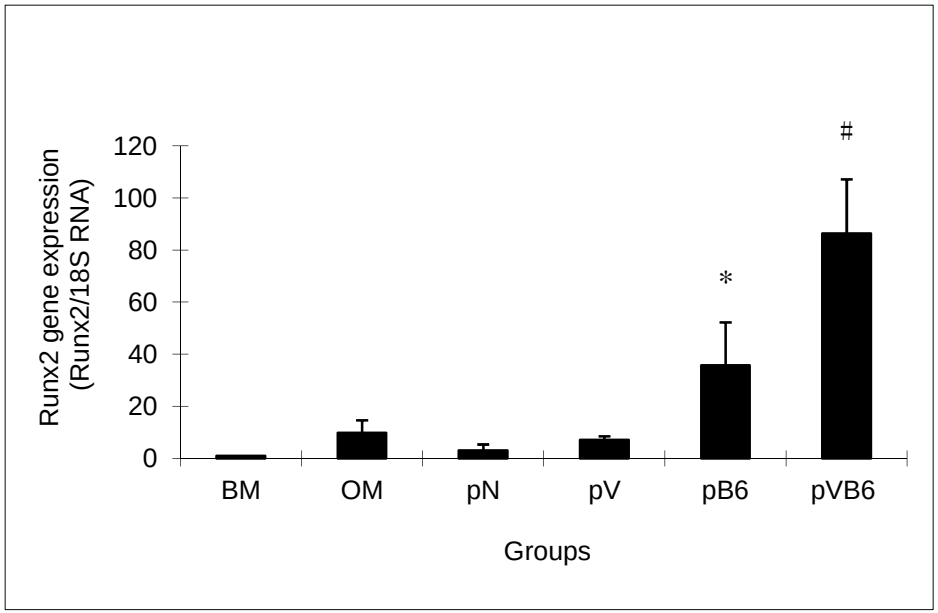

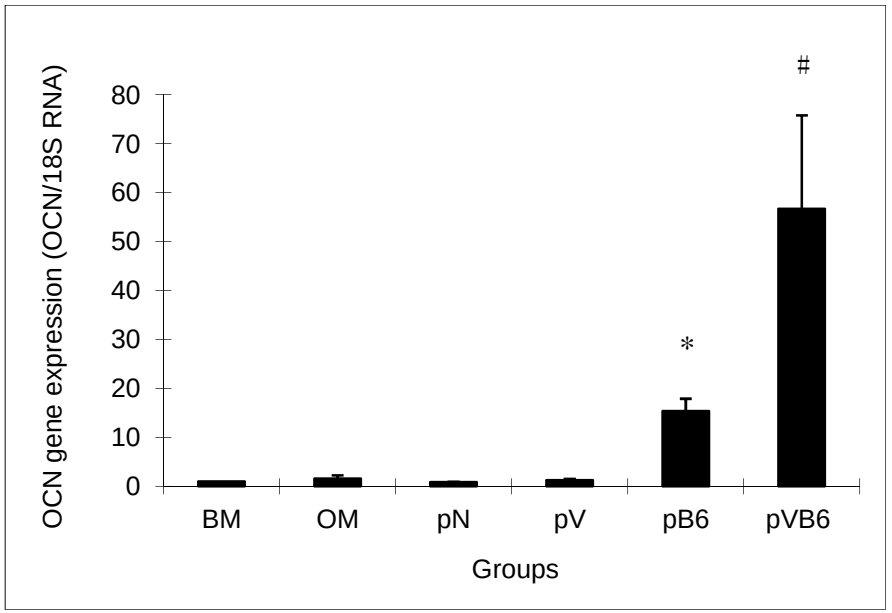

VEGF synergistically enhances BMP-6 induced expression of OCN and Runx2 in D1 cells at day 2. The bars represent the standard deviations of the means. * p < 0.05, # p < 0.01 vs. OM, pN and pV group.

In Vivo Study

Pre-implantation Scanning electron microscopy and confocal images

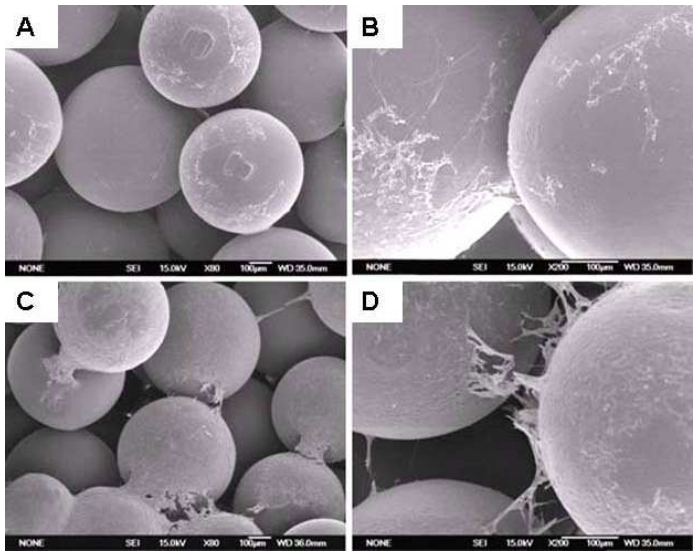

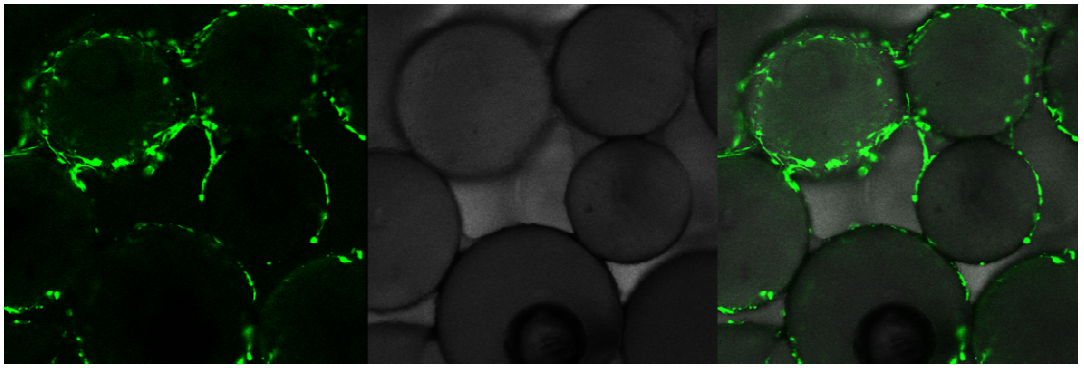

Left: SEM images of D1 cells on the PLAGA scaffolds at day 14 (A ×80 B ×200) and day 21(C ×80 D ×200). Right: Confocal images at day 21(100X).

Results *in vivo*: Micro-CT

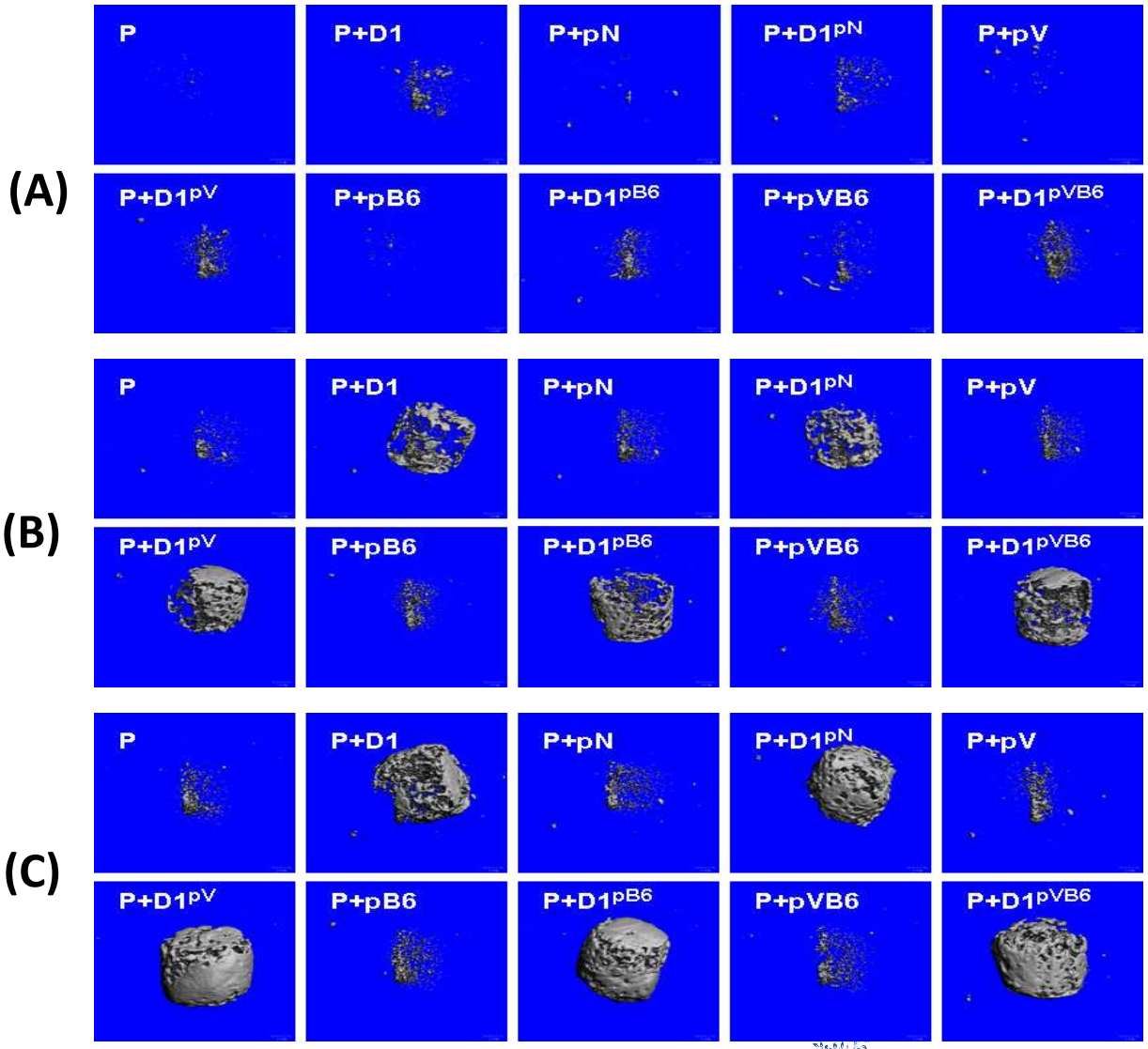

Micro-CT images of the retrieved implants after 2, 3 and 4 weeks showing bone formation on the PLAGA scaffolds. The groups are indicated at the top of each panel. Each group contained four samples, and representative images were shown. **(A)** Two weeks, **(B)** Three weeks and **(C)** Four weeks.

von Kossa staining of retrieved implants

Results *in vivo*

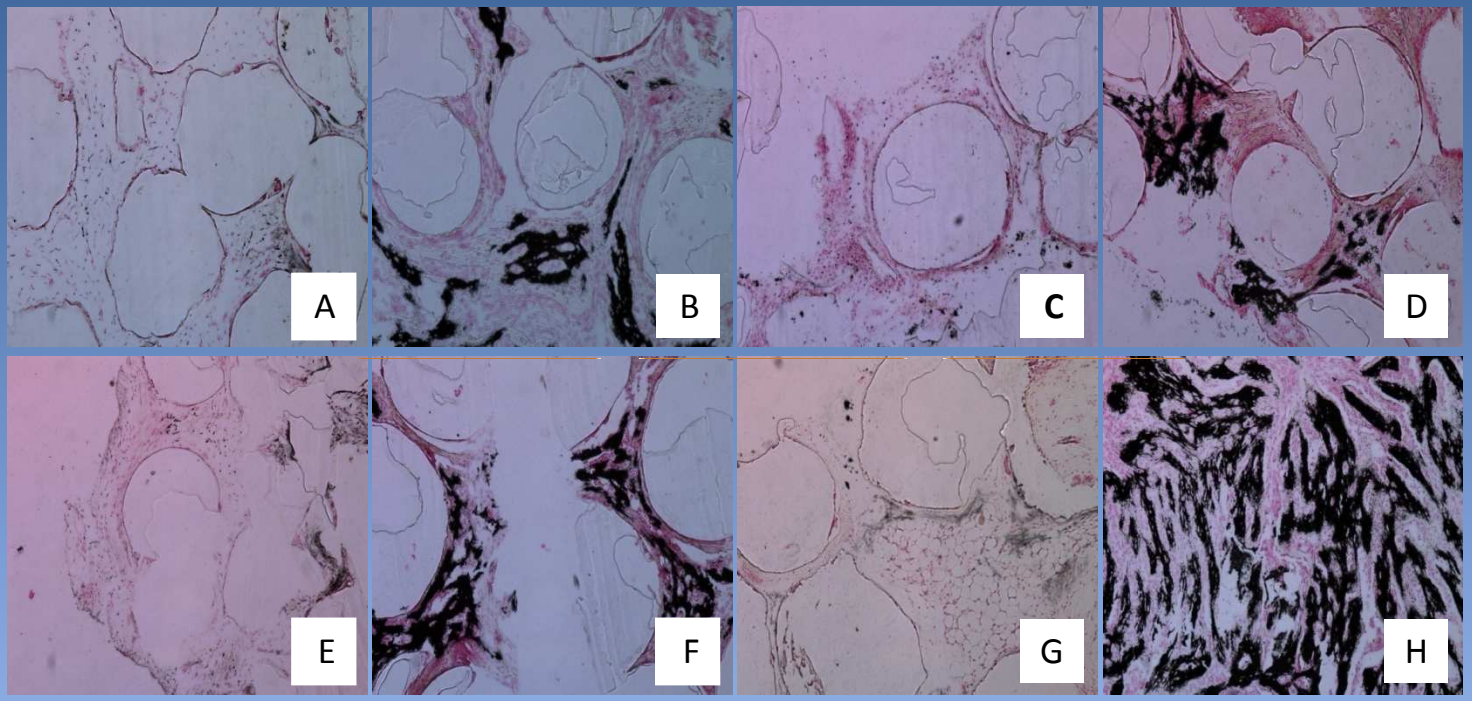

Histological analysis of retrieved PLAGA implants after 3 weeks of implantation using von Kossa staining showing bone formation. (A) PLAGA, (B) PLAGA+ D1, (C) PLAGA + pV, (D) PLAGA+ D1^{pV}, (E) PLAGA + pB6, (F) PLAGA+D1^{pB6}, (G) PLAGA + pVB6, (H) PLAGA+D1^{pVB6} (×100 magnification).

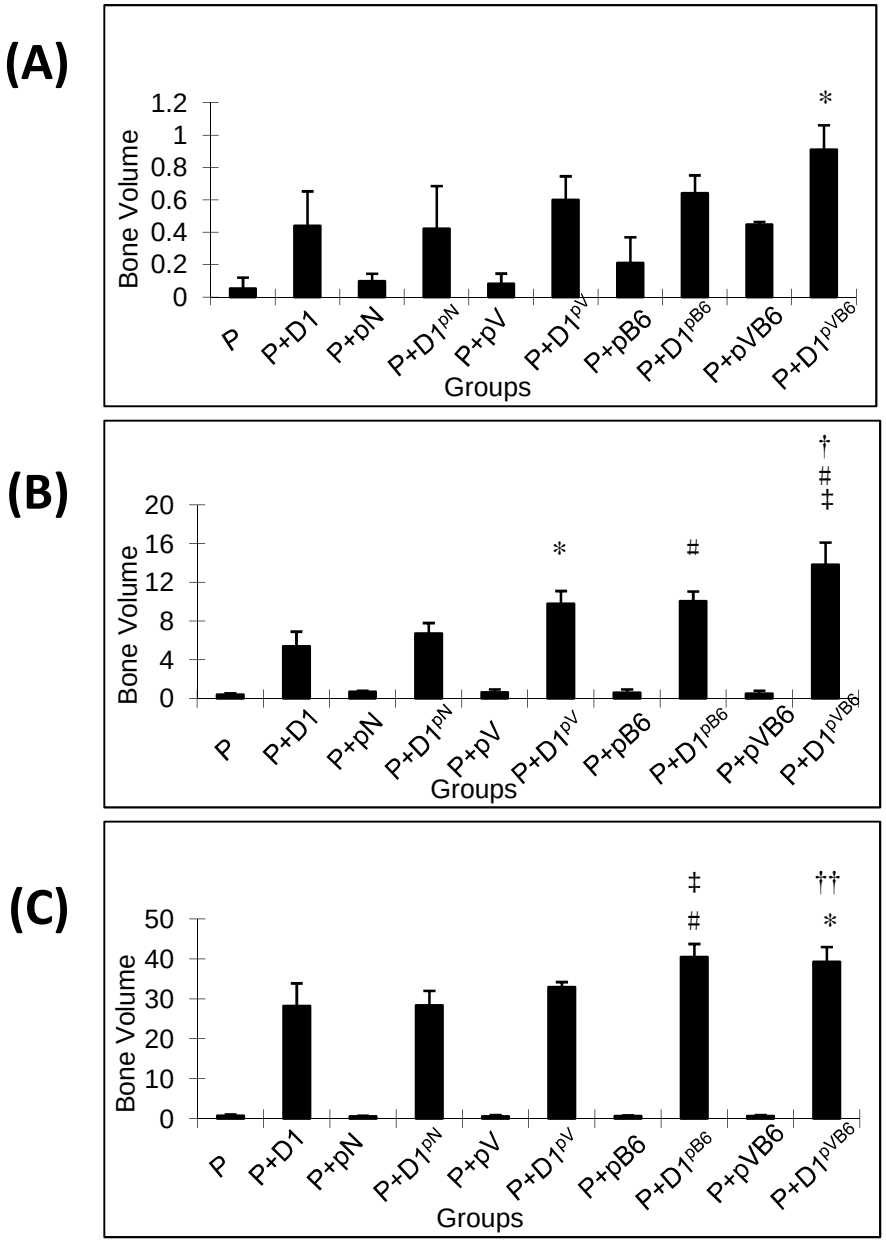

Ectopic bone formation at 2 weeks **(A)**, 3 weeks **(B)**, 4 weeks **(C)** after subcutaneous implantation. Bone volumes were calculated from 3D reconstructed images. The bars represent the means and standard deviations of the means. ‡ $p < 0.01$, †† $p < 0.05$ vs. P+ $D1^{pV}$ and * $p < 0.05$ vs. P+D1 and P+$D1^{pN}$ group; # $p < 0.01$ vs. P+D1 and P+$D1^{pN}$ group; † $p < 0.05$ vs. P+$D1^{pB6}$.

The critical sized mandible defect

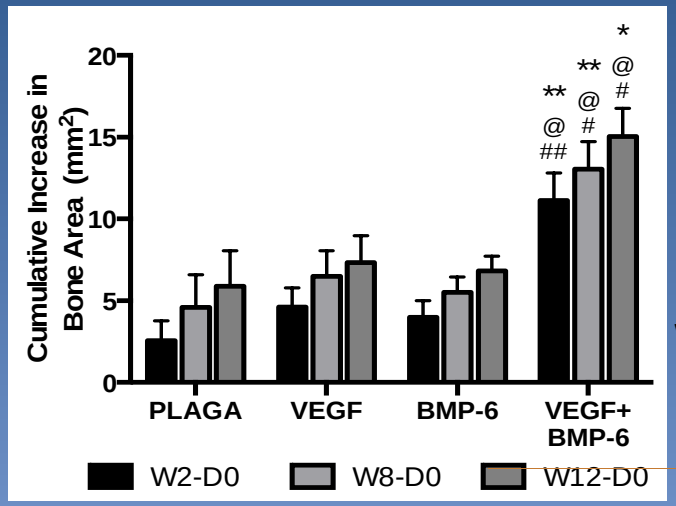

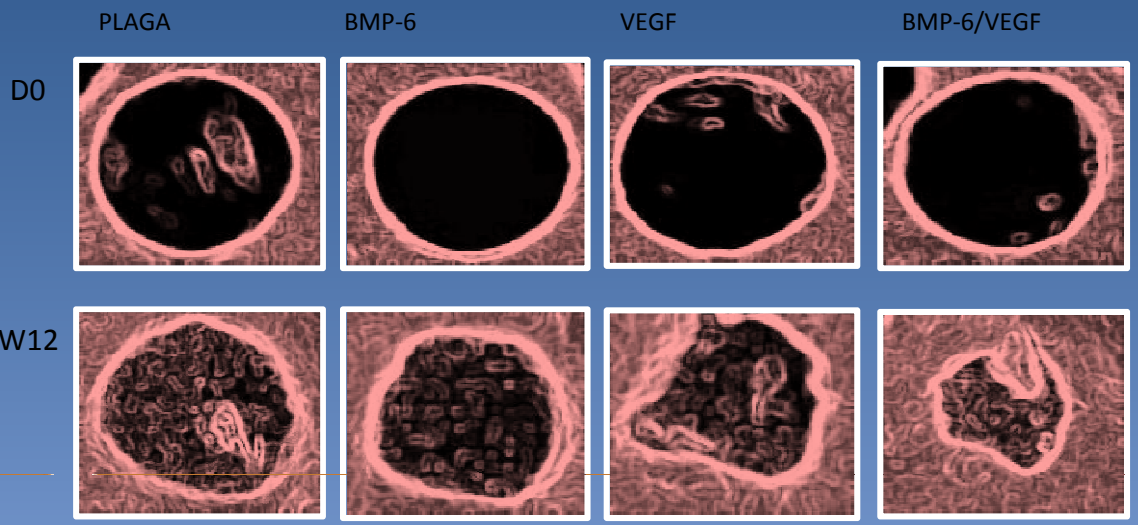

Bone growth in the critical size mandible defect measured using microCT. The left panel shows the cumulative increase in new bone formed measured in mm^3 week 2, week 8 and week 12 after implantation ($p<0.01$ & *$p<0.05$ compared to PLAGA control; $^{\alpha}$ $p<0.05$ compared to VEGF treatment; $^{\#\#}$ $p<0.01$ & #$p<0.05$ compared to BMP-6 treatment at similar time points). The right panel shows representative images of all treatments at day 0 and week 12.**

Vascularization in the critical size Mandible defect measured using microfil enhanced microCT imaging. MicroCT images showing vessel in-growth at week 12 for animals treated with (A) PLAGA, (B) VEGF in PLAGA microspheres (C) BMP-6 in PLAGA microspheres , (D) VEGF+BMP-6 in PLAGA microspheres.

Conclusions

- VEGF showed synergistic interaction with BMP-6 to enhance osteoblastic differentiation of MSCs *in vitro (cloned and mixed rodent bone marrow cells)*.
- The synergistic interaction was also evident *in vivo* in rodents where more bone and vessels were formed.

Question and hypothesis

- Why it works?
- How does the interplay between VEGF and BMP enhance osteogenesis by MSCs ?
- Hypothesis: cross-talk between VEGF and BMP-6 signaling pathways controls osteogenic differentiation of stem cells

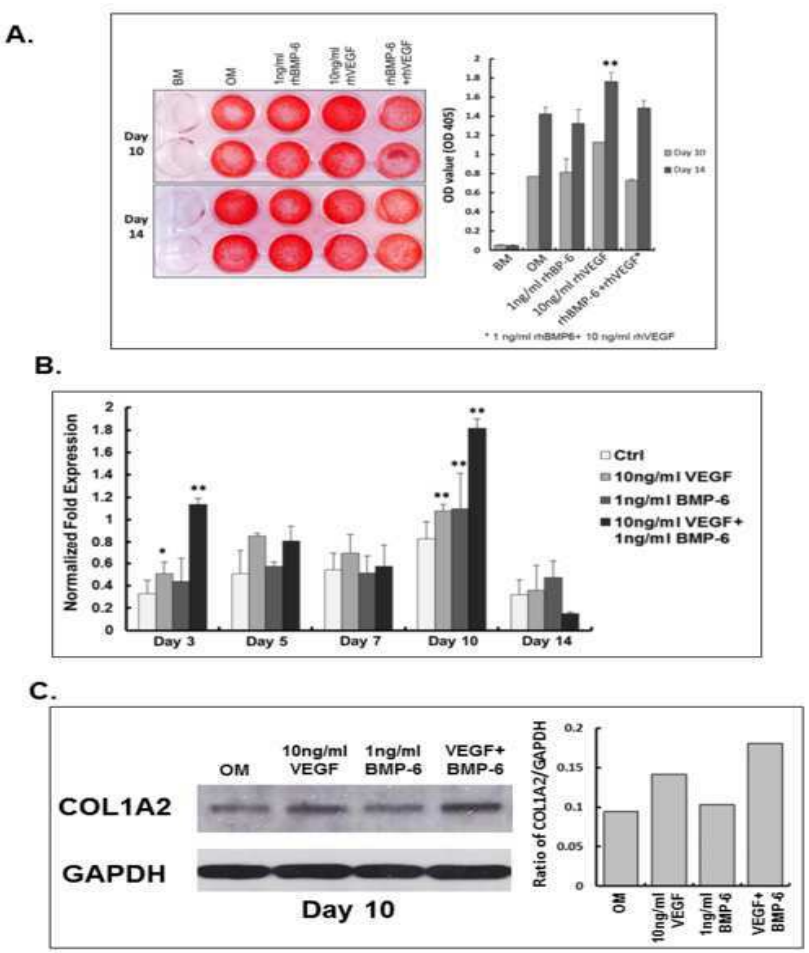

Figure 1. Combination of VEGF and BMP-6 does not increase mineralization but synergistically enhances **COL1A2 mRNA** and protein levels in hADSCs in a temporal fashion. (A). Alizarin Red Staining. (B). Synergistic and temporal enhancement of COL1A2 gene expression. **mRNA** levels were quantified using real time PCR and normalized to 18S rRNA. (C). **COL1A2 protein** level. Western blot showing up-regulation of COL1A2.

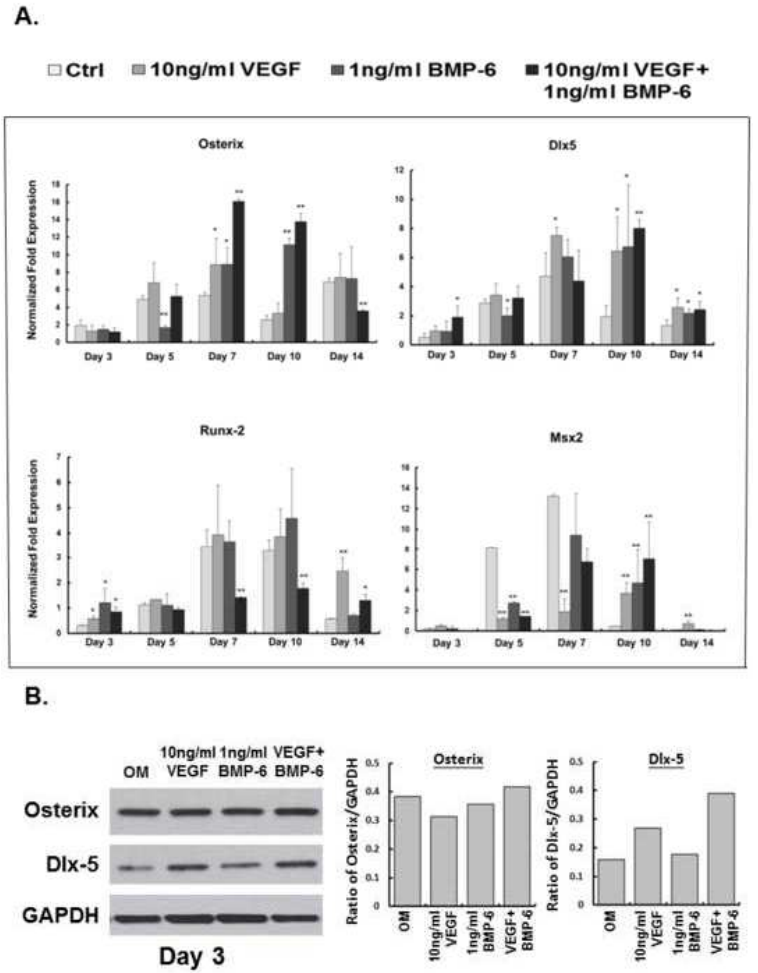

Figure 2. VEGF and BMP-6 up-regulation of COL1A2 in hADSCs correlates with up- regulation of **osterix and Dlx5** but not with runx2 and Msx2 expression. (A, B). Enhanced expression of osterix and Dlx5. mRNA levels were quantified using real time PCR and normalized to 18S rRNA (A). Protein expression was determined by western blot (B).

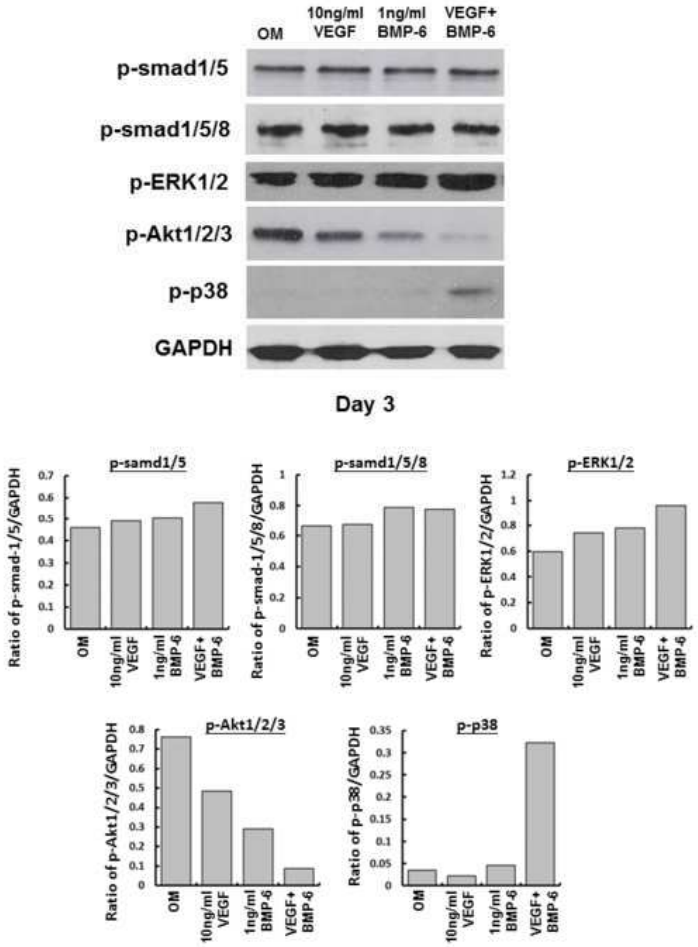

Figure 3. Combination of VEGF and BMP-6 inhibits activation of **Akt** and enhances activation of **p38** in hADSCs.

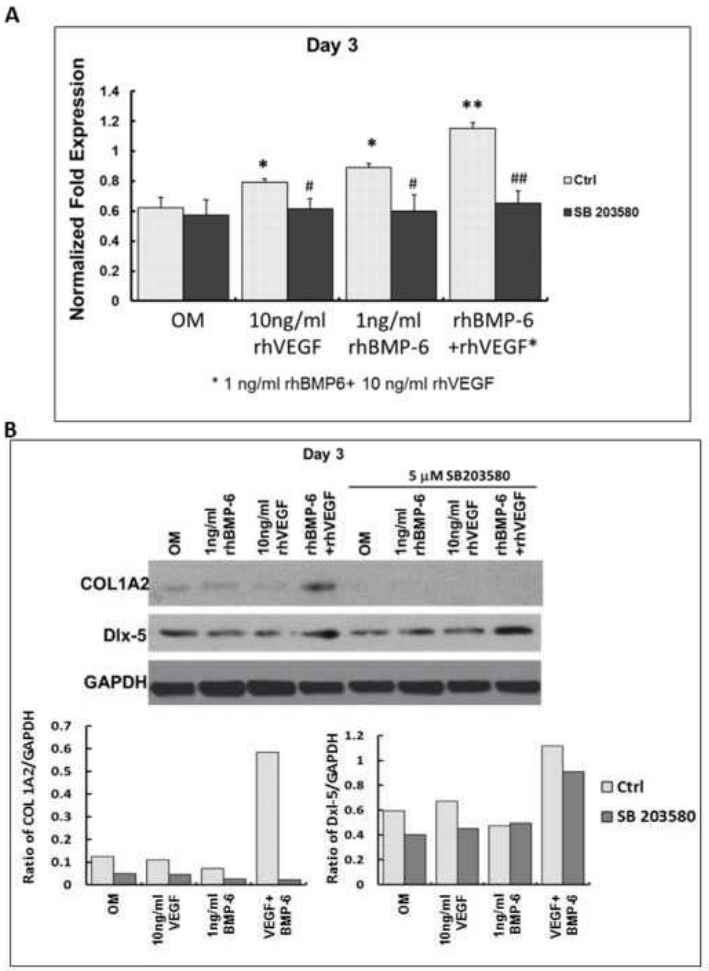

Figure 4. **Inhibition of p38 activation** using SB203580 abrogates cross-talk between VEGF and BMP-6 pathways and prevents up-regulation of **COL1A2** in hADSCs (A). mRNA expression of COL1A2 was determined using real time PCR with 18S rRNA as internal standard (B).

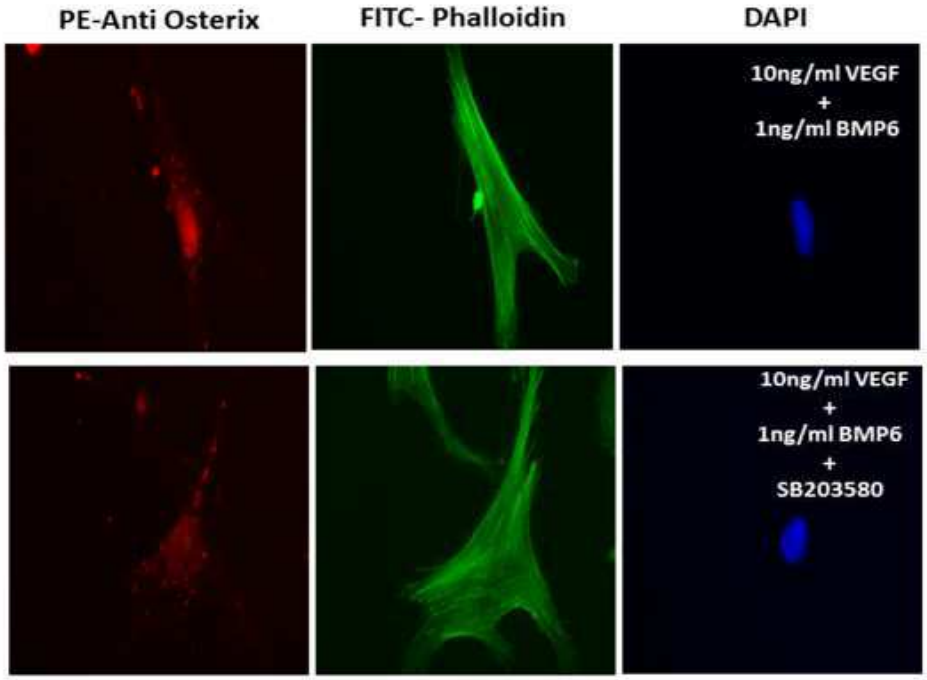

Figure 5. **Inhibition of p38 activation** using SB203580 prevents enhanced nuclear translocation of **osterix** induced by combination of VEGF and BMP-6 in hADSCs. Fluorescence microscopy images after staining the cells with anti-osterix antibody, phalloidin and DAPI after 18 hours of culture with and without p38 inhibitor SB203580.

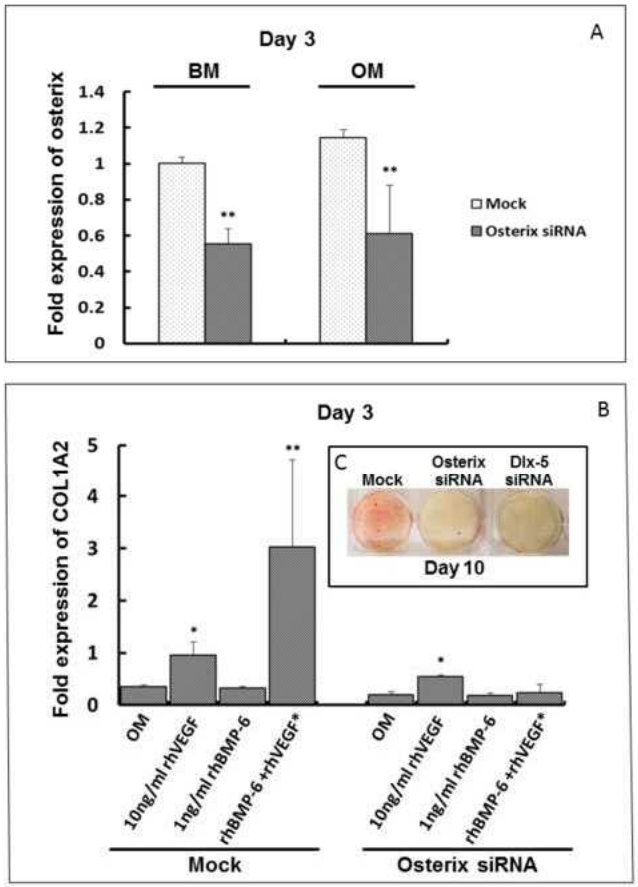

Figure 6. Up-regulation of COL1A2 in hADSCs upon addition of VEGF and BMP-6 requires **osterix** expression. (A**) siRNA knock-out of osterix** in hADSCs grown in BM and OM. (B) COL1A2 expression in hADSCs after osterix knock-out using siRNA. (C) mineralization in hADSCs after osterix or Dlx5 knock-out using siRNAs showing no mineralization.

Loss of function assay

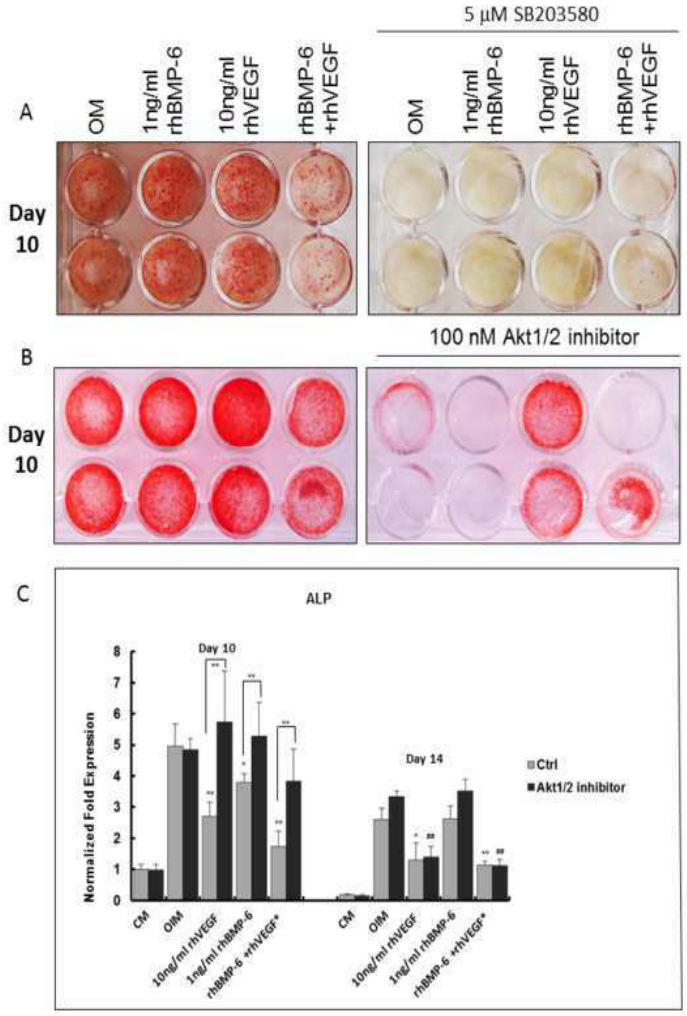

Figure 7. **Inhibition of p38** activation using SB203580 completely inhibits mineralization in hADSCs but **inhibition of Akt** activation only partially affects VEGF plus BMP-6 induced mineralization and enhances ALP gene expression. (A, B) Alizarin Red Staining. hADSCs were grown for 10 days after adding p38 (A) or Akt inhibitor (B) to the culture medium and mineralization was assessed using alizarin red staining and representative images were captured. (C) ALP gene expression increased after addition of Akt inhibitor (at days 10 and 14).

Discussion

- The study demonstrated that the synergistic interaction of VEGF with BMP-6 up-regulates COL1A2

- Increased COL1A2 and mineralization is associated with expression of osterix and Dlx5, as well as activation of p38 and inhibition of Akt

Conclusion

This study for the first time reveals a novel axis controlling osteogenic differentiation of hADSCs through cross-talk between VEGF and BMP-6 signaling pathways that activates p38 but inhibits Akt leading to enhanced osteogenesis by stem cells.

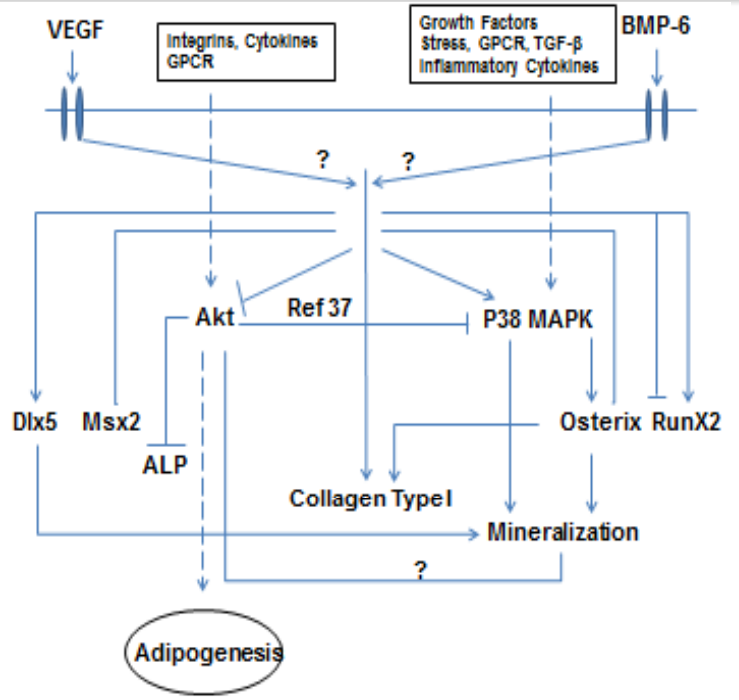

Future goals

- **Application in bone defect model in large animal**
- **Select immunoprivileged MSCs with optimal osteogenesis (collaborated with Drs. Lobo, Brown, Dighe)**
- **Best scaffolds (Collaborated with Drs. Chris Li, Yang)**
- **Optimal combination of growth factors delivered at the right time, dose and location.**

UVA Ortho Research Team